

# Structure and Mechanics of Nonpiscine Control Surfaces

Frank E. Fish

**Abstract**—Animals display a variety of control surfaces that can be used for propulsion and maneuvering devices. For nonpiscine vertebrates, these control surfaces are primarily evolutionary modifications of the paired appendages (i.e., legs). The diversity of control surfaces can be classified with regard to the forces used for stability and maneuverability. For animals, the pertinent forces are pressure drag, acceleration reaction, and lift. These forces can be generated actively by motion of the control surfaces or passively from flows produced by movements of the body or external flow fields. Drag-based control surfaces are associated with paddling and rowing movements, where the limbs are oriented either in the vertical parasagittal plane or horizontal plane, respectively. The paddle is unstreamlined and has a triangular design with a broad distal end, thereby affecting a large mass of water. Appendages, which are used to generate lift-based forces, are relatively stiff hydrofoils. To maximize lift, the hydrofoil should have a crescent wing-like design with high aspect ratio. This shape provides the hydrofoil with a high lift-to-drag ratio and high propulsive efficiency. The tail flukes of cetaceans are streamlined control surfaces with a wing-like design. The flukes of cetaceans function in the hydrodynamic generation of forces for thrust, stability, and maneuverability. The three-dimensional geometry of flukes is associated with the production of lift and drag. Previous studies of fluke geometry have been limited in the number of species examined and the resolution of measurements.

**Index Terms**—Control surface, design, flippers, hydrodynamics.

## I. SURVEY OF ORGANISMS

### A. Nonpiscine Swimmers

**E**XCLUSIVE of fish, the taxonomic list of aquatic animals that use control surfaces for stabilizing the body, maintaining trim, station holding, maneuvering, and propulsion, include amphibians, reptiles, birds, mammals, and cephalopod mollusks. The general morphology of these control surface is remarkably similar to the design of manufactured hydrofoils and propellers. Analysis of the structure and performance of nonpiscine swimmers would be advantageous to engineers in the construction of biomimetic devices.

Within the amphibians, frogs swim using a simultaneous rowing action of the two hind feet, which have become expanded with an interdigital webbing [1], [2]. No analysis has been undertaken to examine maneuverability in frogs.

Within the reptiles, there are a variety of aquatic and semi-aquatic species of turtles (order Chelonia) that use paired appendages for swimming and maneuvering (Fig. 1). Aquatic

Manuscript received September 14, 2003; revised May 14, 2004. This work was supported by the Office of Naval Research under Grant N000140310004, sponsored by Dr. P. Bandyopadhyay.

The author is with the Department of Biology, West Chester University, West Chester, PA 19383 USA (e-mail: ffish@wcupa.edu).

Digital Object Identifier 10.1109/JOE.2004.833213

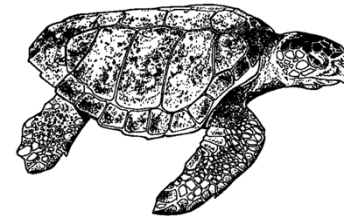


Fig. 1. Sea turtle showing modification of the foreflippers.

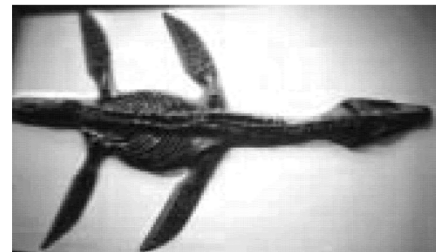


Fig. 2. Plesiosaur skeleton showing wing-like pectoral and pelvic flippers.

propulsion is effected by alternate rowing motions of the four paddle-like feet in semi-aquatic freshwater turtles [3], [4]. For propulsion, sea turtles use a wing-like motion of the two forelegs, which have been modified as flippers [5]–[8].

In addition to extant, swimming reptiles (e.g., sea turtles, order Chelonia, family Protostegidae), there were a number of aquatic groups that occurred at a time when dinosaurs inhabited the earth (245–65 million years ago) and have since become extinct. These marine reptiles grew to large body sizes and included ichthyosaurs (order Ichthyosauria), mosasaurs (order Squamata, family Mosasauridae), plesiosaurs and nothosaurs (order Sauropterygia), and placodonts (order Placodontia) [9], [10]. The ichthyosaurs used body and tail undulations to swim. In early ichthyosaurs, the propulsive movements were eel-like, but more derived species developed a high aspect ratio (AR) tail and fusiform body that were analogous with respect to swimming motion and habits to sharks and dolphins [11]–[15]. Highly derived species of ichthyosaurs had paired pectoral and pelvic flippers and a dorsal fin resembling the control surfaces of modern dolphins. Mosasaurs were elongate aquatic lizards that ranged in size from 4 to 15 m long. Mosasaurs swam by undulation of a long broad tail. Paddle-like pectoral and pelvic appendages were present and may have functioned in maneuvers. Swimming by plesiosaurs is the least understood, because these animals lack modern relatives with similar anatomical designs and habits. The body was highly fusiform, although slightly compressed, with the head being large with a short neck or small with a long neck (Fig. 2). The fore and hind limbs

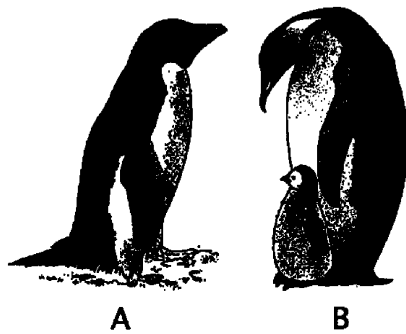


Fig. 3. Penguins. (A) Adélie penguin and (B) Emperor penguin.



Fig. 4. Sea otter showing paddle-like hind feet.

were modified as high aspect-ratio wing-like flippers [16]–[20]. It is believed that plesiosaurs swam with wing-like motions rather than rowing or paddling, but the pattern of movement between the four limbs is unknown.

A number of bird species are cable of swimming, including penguins (order Sphenisciformes); loons (order Gaviiformes); grebes (order Procellariiformes); pelicans and cormorants (order Pelecaniformes); ducks, geese, and swans (order Anseriformes); and gulls, auks, and puffins (order Charadriiformes). The dominant form of swimming is paddling at the water surface. Paddling uses alternate strokes of the webbed hind feet, as exemplified by ducks [21]–[23]. Winged swimming is used by puffins and penguins. Puffins and their relatives use the wings for both swimming and flight [24]. In penguins, the wings are used exclusively for swimming and have taken on a high AR design (Fig. 3) [25]–[29].

A variety of mammalian lineages have secondarily invaded the water (Figs. 4–6) [11], [30]. Highly derived aquatic mammals are found in the taxonomic orders Cetacea (whales, dolphins, and porpoises), Pinnipedia (seals, sea lions, fur seals, and walrus), and Sirenia (manatees and dugong). The cetaceans are divided into two groups, the baleen whales (Mysticete) and toothed whales (Odontocete). Less derived mammals that have lifestyles tied to the water are semi-aquatic from a wide range of mammalian orders, including Monotremata (platypus), Marsupialia (water opossum), Insectivora (water shrew, desman, and otter shrew), Carnivora (otters and polar bear), Rodentia (beaver, muskrat, and nutria), Lagomorpha (marsh rabbit), Perissodactyla (tapir), and Artiodactyla (hippopotamus). Most semi-aquatic mammals swim by paddling or rowing with webbed feet (Fig. 4) [30]. Paddling is confined to swimming at the surface, whereas rowing motions are used when submerged to aid in thrust production and dynamic buoyancy control [31]–[37]. Typically, the pelvic appendages are used by semi-aquatic mammals for propulsion and maneuvering. The pectoral limbs are used for swimming and turning in water by the polar bear. The platypus rows using its webbed forelimbs

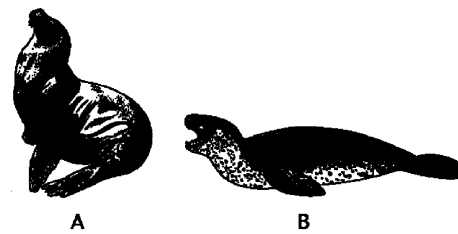


Fig. 5. Pinnipeds showing the difference in pectoral and pelvic flippers for (A) the Otariid sea lion and (B) the Phocid leopard seal.

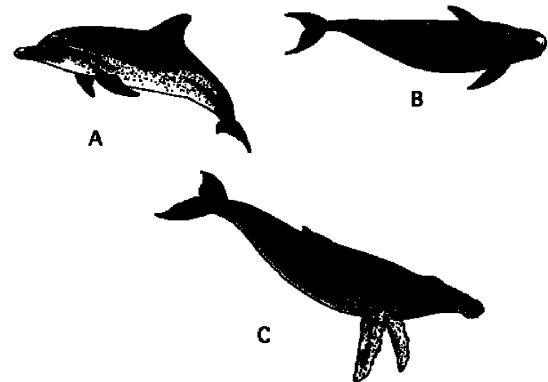


Fig. 6. Cetaceans exhibiting control surfaces of the pectoral flippers, dorsal fin, caudal peduncle, and caudal flukes. (A) Spotted dolphin, (B) pilot whale, and (C) humpback whale.

[34], [37]. Although propulsion is mainly produced by paddling and undulation of the hind feet and tail, respectively, in river otters (*Lutra canadensis*), the forelimbs are used during maneuvers [38].

Marine mammals, including the orders Pinnipedia, Cetacea, and Sirenia, are the most adapted to the aquatic environment. The control surfaces of marine mammals are used for propulsion and maneuvers (Figs. 5 and 6; [12], [30], [39]–[45]).

The foreflippers used by the pinnipeds (e.g., sea lions) act as oscillatory hydrofoils [37]. Both fore and hind flippers (Fig. 5) are used for turning [46]. Lift-based oscillations also generate thrust from dorsoventral movements by the caudal flukes of cetaceans and sirenians [47]–[51] or from lateral movements of the paired hind flippers by the Phocidae and Odobenidae [41], [52]–[55]. Lift-based oscillation, exclusive of the otariid pinnipeds, is analogous to the thunniform mode of fishes that represents the advanced end of a continuum of undulatory swimming modes [56], [57]. In this mode, undulations of the body are transmitted to the oscillatory hydrofoil through mobile joints. These joints control the angle of attack of the hydrofoil to maintain lift and thrust throughout the stroke cycle [41], [56].

For cetaceans, the control surfaces consist of the pectoral flippers, dorsal fin, compressed caudal peduncle, and caudal flukes (Fig. 6). The pectoral flippers, caudal peduncle, and caudal flukes are mobile and provide the main contribution to lateral turning, diving, and surfacing [58]–[62]. The broad peduncle and flukes at the end of the tail serve collectively as a rudder for turning. During turns, the tail can be twisted rotating the flukes up to  $88^\circ$  [62]. Dorsal fins are not mobile. The position of the dorsal fin aft of the center of gravity (CG) is important for stability [47], [63], [64]. The fin resists yawing

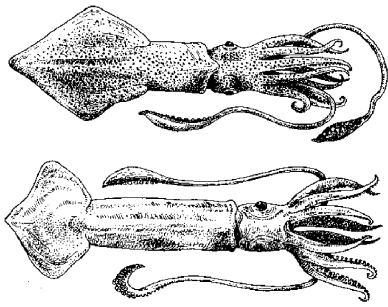


Fig. 7. Squid displaying lateral fins.

and rolling and acts to prevent side-slip during turning maneuvers [62]. The beluga whale (*Delphinapterus leucas*) lacks a dorsal fin and turns by rolling the body by  $90^\circ$  [62].

Sirenians, including manatees and dugongs, have few control surfaces with only two mobile pectoral flippers and the tail fluke. These herbivorous mammals are generally slow moving [48]. Manatees are able to precisely maneuver using the mobile paddle-like pectoral flippers in combination with an ability to hydrostatically control body trim [65].

Convergent with the control surfaces exhibited by various aquatic vertebrates, cephalopod mollusks display a range of fins that can act to stabilize the animal trajectory (Fig. 7). In various species, the fins can be undulated for propulsion at low speeds, whereas high-speed swimming is performed by jet propulsion [66]. When jetting, the fins typically are positioned anteriorly. The arms can also be used as control surfaces to provide lift for directional control [66]. During attacks on fish, the orientation may be reversed with the fins posteriorly situated. These head-first attacks have maximum speeds of 2.4–2.6 m/s with accelerations up to  $5.6 \text{ m/s}^2$  [67]. In flying squid, the fins are used as canards in concert with the laterally extended arms during gliding flight [68].

### B. Paddle versus Hydrofoil

The diversity of control surfaces can be classified with regard to the forces used for stability and maneuverability. For animals, the pertinent forces are pressure drag, acceleration reaction, and lift [30], [42], [69]–[71]. These forces can be generated actively by motion of the control surfaces or passively from flows produced by movements of the body or external flow fields.

Pressure drag is a result of the asymmetry of the fore and aft flow around an appendage. This asymmetry creates a pressure difference that is the basis of the drag. Drag-based control surfaces are associated with paddling and rowing movements, where the limbs are oriented either in the vertical parasagittal or horizontal plane, respectively. The paddle is unstreamlined and has a triangular design with a broad distal end, thereby increasing propulsive efficiency by affecting a large mass of water [72], [73]. In addition, the narrow attachment of the triangular paddle with the body reduces drag due to interference between body and propulsor. The paddle has a stroke cycle that is divided into power and recovery phases [2], [36], [74]. During the power phase, the paddle is swept in a direction opposite to the direction of the drag vector. Depending on the direction of motion, the paddle can be used to provide an anterior thrust,

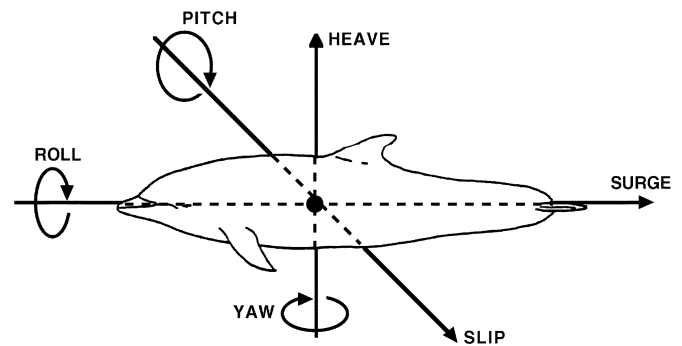


Fig. 8. Translational and rotational degrees of freedom. The position of the center of gravity (CG) is indicated by the solid circle. Rotational and translational instabilities associated with a three-dimensional (3-D) axis system are projected on the lateral view of the dolphin. Translational motions include movement along the three axes as surge (X-axis), heave (Y-axis), and slip (Z-axis). Rotational motions include roll (rotation around the X-axis), pitch (rotation around the Y-axis), and yaw (rotation around the Z-axis).

a braking action, reversal of swimming direction, or a turning moment if used asymmetrically. The recovery phase repositions the appendage. To prevent an oppositely applied pressure drag on the paddle that will negate the force and movement generated, the paddle is collapsed or feathered (Fig. 8). Examples of drag-based paddlers include labriform fish, frogs, turtles, ducks, semi-aquatic mammals, and manatees. Paddling is associated with slow surface swimming and precise maneuverability.

Acceleration reaction results from changes in the kinetic energy of water accelerated by action of the propulsive body structure [70], [75]. The acceleration reaction is dependent on an additional inertial mass, which is the added mass that when added to the inertia of the body accelerating in the water balances the momentum changes [75], [76]. The acceleration reaction differs from drag in that: 1) the acceleration reaction is directly proportional to the volume of an object, while drag is proportional to the surface or cross-sectional area and 2) the acceleration reaction depends on changes in velocity of an object, resisting both acceleration and deceleration, while drag depends on the instantaneous velocity of the object, resisting acceleration but augmenting deceleration [75]. Some resistive drag accompanies this mode of force generation due to viscous effects. Animals that swim by undulation of appendages (Ostraciiform, Gymnotiform, Balistiform, Rajiform, and Diodontiform fish) use the acceleration reaction [56], [70], [76], [77]. Flattening of the undulatory surface enhances the magnitude of inertial effects [12], [78]–[80]. Control surfaces using undulations are typically broad based [56], [57]. Because undulations can be continuously generated by the swimmer, force production is constant.

Use of the acceleration reaction is constrained by size [70]. As animals get larger, the ability of the muscle to generate force relative to inertial forces decreases [76].

Acceleration reaction is also used for jet propulsion [75]. Thrust results from the forceful expulsion of a mass of water from some internal cavity. Squids are capable of some maneuvering control by directing the jet.

Appendages, which are used to generate lift-based forces, are relatively stiff hydrofoils. To maximize lift, the hydrofoil should have a crescent wing-like design with high AR ( $\text{span}^2/\text{area}$ ) [78], [81], [82]. This shape provides the hydrofoil with a high

lift-to-drag ratio and high propulsive efficiency [83]. Hydrofoils can be held stationary at various angles of attack or oscillated ([12], [40], [41], [43], [85]–[87]). The angle of attack generally is a small angle corresponding to the deflection of the hydrofoil from the flow. Lift arises from asymmetries in the flow. The asymmetry generates a pressure difference between the sides of the hydrofoil with a net force normal to the incident flow. Lift is generated continuously with a steady flow. Although some resistive drag is produced by the hydrofoil, it is small compared to the lift. The high lift-to-drag ratio is a function of the high AR of the hydrofoil [30], [39], [41], [56], [85], [86]. Lift-based appendages to control direction are used by tuna, sharks, sea turtles, penguins, cetaceans, sea lions, and phocid seals.

The performance of the drag- and lift-based propulsive systems are limited by swimming speed. Drag-based paddling operates most effectively at low speeds, whereas lift-based hydrofoils perform best at higher speeds. As a flow field needs to be established for a lifting surface to work, hydrofoils are limited in use to conditions where the body of an animal is already in motion. Paddles can be used when the body is stationary. A large-area paddle can impart sufficient momentum to a mass of water to induce a recoil in a stationary body. The reaction force can be used to accelerate the body and produce a maneuver. Because the thrust production by the paddle is dependent on its movement in the direction opposite the body movement, thrust decreases as the velocity of the body increases. At a speed where the body and paddle speeds are equivalent, thrust can no longer be produced [88].

## II. LOCATION OF CONTROL SURFACES IN RELATION TO STABILITY

### A. Degrees of Freedom

Aquatic animals have six degrees of freedom: three translational (heave, slip, and surge) and three rotational (yaw, pitch, and roll) directions (Fig. 8) [89]. Movement in any of these degrees of freedom represents an instability. Stability about the roll axis is lateral stability, about the yaw axis is directional stability, and about the pitch axis is longitudinal stability [90]. The position, size, and geometry of the control surfaces help to maintain stability and regulate instabilities, as required in maneuvering [62], [81], [91]–[102].

### B. Stability Parameters

Features associated with the placement and design of control surfaces provide stability by producing torques in response to changing flow direction [59], [62], [81], [91], [92], [101], [103]–[105]. Control surfaces located far from the CG can generate large directionally correcting torques, because of their long lever arm. Propulsors arranged around the CG are postulated to promote maneuverability [100]. The relative size of the control surface in relation to its location also will determine the magnitude of the torques [59].

Stable movement occurs with posterior placement of the control surfaces relative to the CG [103]. This placement positions the CP aft of the CG. The reverse position will create an unstable situation. Perturbations would result in tumbling. Placing

the tail fin well aft of the CG turns the body into the flow in a manner similar to a weathercock [89].

Both dihedral and sweep of the control surfaces act similarly to stabilize roll and yaw, respectively [56], [91], [92], [106], [107]. Dihedral is a tilting of the control surface relative to the body and sweep is rearward sloping of the leading edge of the control surface. Dihedral is good at resisting side slip and yaw [90]. Because the velocity of a fluid-oriented obliquely to the trajectory of the arrow encounters each member of a paired control surface differently, the control surface with a more perpendicular orientation to the flow will generate larger forces than the other control surface and will produce stabilizing moments [90]. Rearward sweep results in a backward shift in the center of lift, providing increased stability [91]. Alternatively, forward swept control surfaces increase maneuverability [108]. Swept wings can be combined with negative dihedral, also called anhedral, to combat coupled instabilities of yaw and roll [89], although anhedral is considered to be destabilizing in aerial flight [108]. Reduced motion of the control surface and reduced flexibility of the body restrict self-generated perturbations [101], [102], [109].

The same features that control stability for an arrow are present in the morphology of animals. Unlike the arrow, the animal body is responsible for producing its own propulsive forces. Flexibility of the body and the appendages, by undulation and oscillation, are necessary in the generation of thrust [42], [56], [78]. These propulsive motions produce transverse recoil forces that must be balanced along the body to maintain stability and minimize energy expenditure during locomotion [78], [110]. The increased flexibility for propulsion can produce its own destabilizing perturbations. The various forms of cyclical and symmetrical movements of the body and appendages can act as dynamic stabilizers [87], [111], [112]. When symmetrically applied, the time-averaged propulsive forces maintain an animal on course, although oscillations in the body are apparent. In elongate animals, recoil forces are balanced by multiple body flexures [56], [73]. However, the animal pays a penalty in terms of increased drag [78]. Animals with short or inflexible bodies reduce recoil by changes in the distribution of the projected area in the direction normal to flexure [59], [78].

## III. MORPHOLOGY OF CONTROL SURFACES

### A. Structural Components and Mobility

The control surfaces, comprising the hydrofoils (flippers) and paddles of nonpiscine vertebrates, are modifications of the limbs of terrestrial animals, which have become adapted for use in water. Both flippers and paddles, therefore, have the same structural elements (i.e., bones) as found in their terrestrial ancestors. Paddles are largely unmodified. Because paddles are used predominately by semi-aquatic animals, they must function for both aquatic and terrestrial locomotion.

Pectoral limbs have a single proximal humerus, which articulates at the shoulder joint with a broad scapula (Fig. 9; [11], [28], [113]–[116]). In reptiles and birds, the shoulder joint also includes the coracoid. In mammals, the humerus has a ball-and-socket articulation with the scapula. The globular head of the

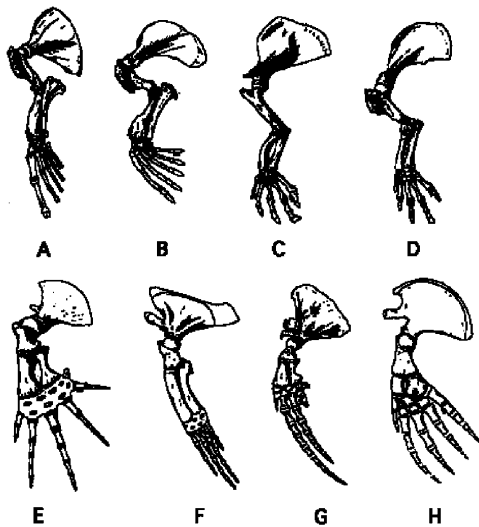


Fig. 9. Skeleton of left pectoral limbs of aquatic mammals including (A) sea lion, (B) seal, (C) manatee, (D) dugong, (E) right whale, (F) blue whale, (G) pilot whale, and (H) river dolphin. From [11], with permission of the publisher.

humerus fits into a concavity on the scapula, which is known as the glenoid cavity. Cetaceans also may involve the sternum in the joint cavity [61]. Distally, the humerus articulates with a preaxial radius and a postaxial ulna. The ulna and radius terminate at the wrist joint and articulate distally with a number of carpal bones. The carpals are followed distally by a set of metacarpals and then the phalanges. The phalanges would comprise the digits in terrestrial animals. As in the terrestrial condition, there are five digits, with the exception of large whales in the family Balaenopteridae, which lack a thumb [117], and birds, which lost digits in the evolution of the wing for flight. In flippers, the digits are not separated. The number of phalanges in each digit of the flipper is variable between species. Hyperphalangy is the condition in which the maximum number of phalanges exceeds the terrestrial number [11]. Hyperphalangy is found in cetaceans and ichthyosaurs.

The appendicular bones of semi-aquatic and aquatic nonpiscine vertebrates differ in proportions from those of terrestrial relatives. Bones of the limbs are robust to accommodate greater muscular and hydrodynamic forces (Fig. 9) [11], [116]. The humerus is short to increase mechanical advantage. The distal bones of paddle-like feet and flippers are elongate [118]. Elongation of the digits increases the surface area of the limb.

Paddle-like limbs of semi-aquatic vertebrates show a degree of mobility that is similar to those of their terrestrial relatives. Despite the number of bony elements and joints within pectoral flipper, mobility between the joints is constrained in more aquatically derived animals. The flipper is made stiff by layers of fibrous connective tissue. For sea turtles, penguins, seals, and sea lions, there is some flexibility at the elbow, which acts as a hinge joint [114]. In seals and manatees, movement at the elbow occurs when these animals paddle [48], [52]. Otherwise, flexion and extension of the elbow is used primarily during terrestrial locomotion by sea turtles and pinnipeds [8], [52].

Movement of flippers occurs primarily at the shoulder joint. This joint is multiaxial, permitting various movements, including protraction, retraction, adduction, abduction, and

rotation [5], [8], [11], [25], [28], [40], [48], [52], [58], [60], [61], [114], [119], [120]. The range of movements at the shoulder varies between taxonomic groups. Animals that use the pectoral appendages to generate propulsive forces display the least limitation in flipper movement. These animals, which include sea turtles, penguins, and pinnipeds, can raise the tips of their forelimbs above the horizontal plane of the body [7], [8], [28], [119]. Penguins can raise their wings to an angle  $45^\circ$  above the horizontal plane [28]. The use of the flippers for paddling in manatees necessitates a high degree of mobility at the shoulder [48]. Pinnipeds use the flippers for aquatic propulsion, but mobility of the joints in the flipper also will be associated with the terrestrial locomotion.

The flippers of cetaceans are positioned on the animal with anhedral. The flippers generally are constrained in their movements. Reduced motion of the flippers of fast-swimming dolphins is necessary to enhance stability [62], [101]. Beaked whales are an exception, with small narrow flippers that can be rotated and adducted to be tucked into slight depressions on the side of the body [121]. This ability may be a mechanism to reduce drag when swimming. Beaked whales are deep (1000 m) and long-diving (1 h) cetaceans and may forgo maneuverability for reduced energy consumption. Humpback whales (*Megaptera novaeangliae*) have long flippers with high mobility. The humpback flipper can be rotated around its long axis by  $120^\circ$  [60]. A tethered whale was able to use the flippers to move the body up, down, forward, backward, and sideways [60].

The mobility of the flippers of fast swimmers appears to be more constrained as compared to the flippers of slow-swimming highly maneuverable animals [11], [60], [61], [101], [122], [123]. The shoulder musculature of *Inia geoffrensis* is highly differentiated in contrast to the faster swimming *Lagenorhynchus*, *Phocoena*, and *Tursiops* [61]. *Inia* is capable of performing a turn with radius that is 10% of its body length [101]. This degree of maneuverability is necessary to operate in the complex environment of a shallow river habitat. Similarly, *Megaptera* uses its long mobile flippers to maneuver in coastal waters for prey [60], [124], [125].

The amount of muscle within flippers is small. Muscles are confined largely toward the shoulder (Fig. 10). The reduction in muscles distally in the limb are the result of reduced lateral motion of the digits. Semi-aquatic animals with little specialization of the limb have muscles that extend into the digits. Muscles associated with upward (adduction) or downward (abduction) movement of flippers insert on the humerus from the sternum, vertebrae, scapula, and clavicle. The major muscle on the ventral side of the animal is the pectoralis; on the dorsal side, the trapezius and latissimus dorsi. Muscles originating at the scapula can rotate the limb.

## B. Streamlining and Associated Hydrodynamic Parameters

1) *Planform*: Flipper planforms vary from elongate wing-like forms in a humpback whale (*Megaptera novaeangliae*; Fig. 11), sea lions, penguins, and sea turtles to rounded paddle-like forms in killer whales (*Orcinus orca*) and beluga whales (*Delphinapterus leucas*). The humpback whale has the longest flipper of any cetacean with length varying from

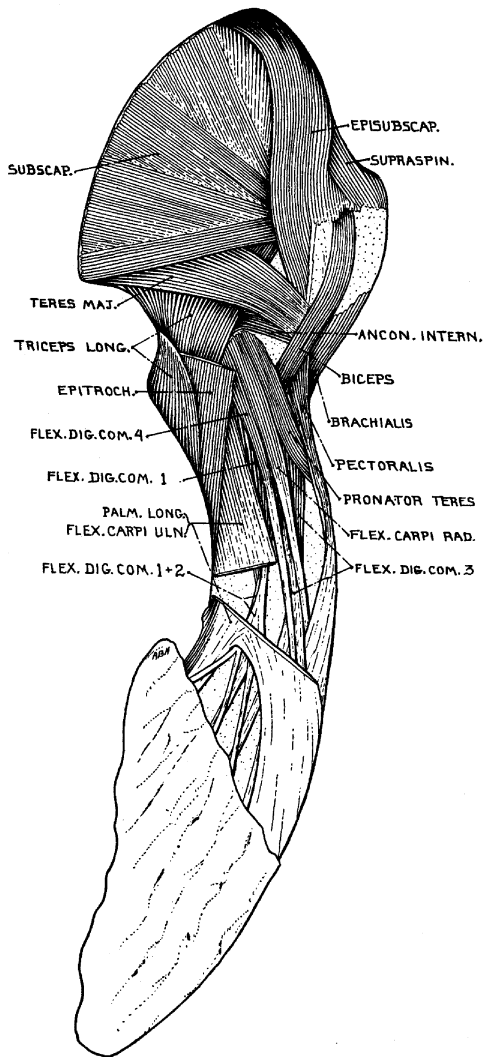


Fig. 10. Musculature of the medial aspect of the left pectoral flipper of a sea lion (*Zalophus californianus*). The bulk of muscle is located proximally in the limb with tendinous and ligamentous connections in the distal part of the flipper. From [11], with permission of the publisher.

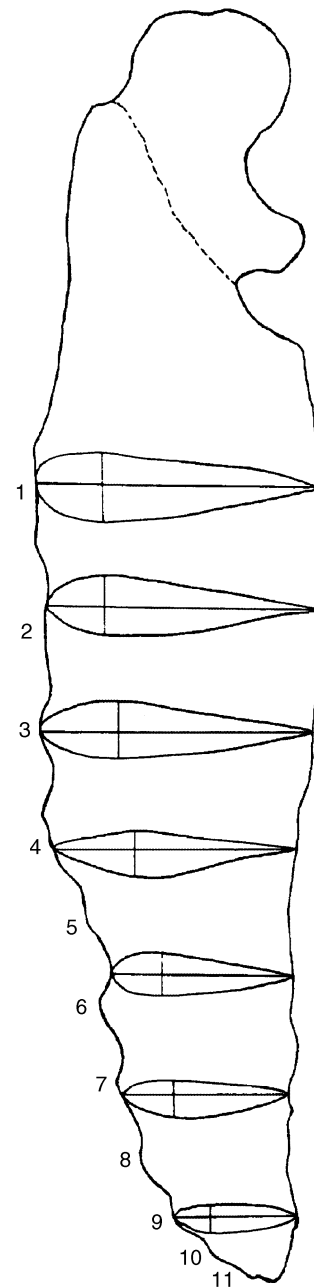


Fig. 11. Flipper planform for *Megaptera novaeangliae*, showing representative cross-sections. The flipper is oriented with its distal tip pointed down. Horizontal lines through each cross-section represent the chord length and vertical lines represent the maximum thickness. Numbers located along the leading edge indicate the center for each of the tubercles. From [125].

25%–33% of body length [60], [126], [127]. The flippers of other cetaceans are no longer than 0.14 body length [60]. For odontocete cetaceans, flipper length directly increases with increasing body length (Fig. 12).

A novel feature on the leading edge of the humpback whale flipper is the presence of 10–11 prominent rounded tubercles (Fig. 11; [125]). The tubercles are large near the body, but decrease in size toward the tip of the flipper. The distance between the tubercles varies from 1.7% to 12.3% of flipper span at the tip and toward the body, respectively. The intertubercular distance is a relatively uniform between 6.5%–8.6% of span over mid-span of the flipper.

When present in cetaceans, dorsal fins are falcate, triangular, or rounded shapes [128]. Dorsal fin height is directly related to body length (Fig. 12). The largest dorsal fin (1.8 m high) is found in male killer whales (*Orcinus orca*) and is a distinct sexual dimorphic characteristic in this species. The dorsal fin is typically swept (Fig. 13) with a maximum reported value of  $66.2^\circ$  [45]. No association between swimming speed and dorsal fin design has been found. Finless whales, such as *Lissodelphis*,

are considered to be a rapid swimmers [129], whereas the beluga (*Delphinapterus leucas*) is reported to be a slow swimmer [43], [44].

The planform of paddle-like feet of semi-aquatic animals is circular or triangular with the narrowest part of the paddle at the base (Fig. 14). The addition of interdigital webbing or fringe hairs on the toes increases the paddle surface area [11]. During the power phase of the paddling cycle, the toes are spread (abducted) to maximize propulsive surface area. During the recovery phase of the stroke cycle, the toes are pulled together (adducted) and flexed to reduce the paddle area. The difference in area of the foot negates a loss of thrust and reduced efficiency

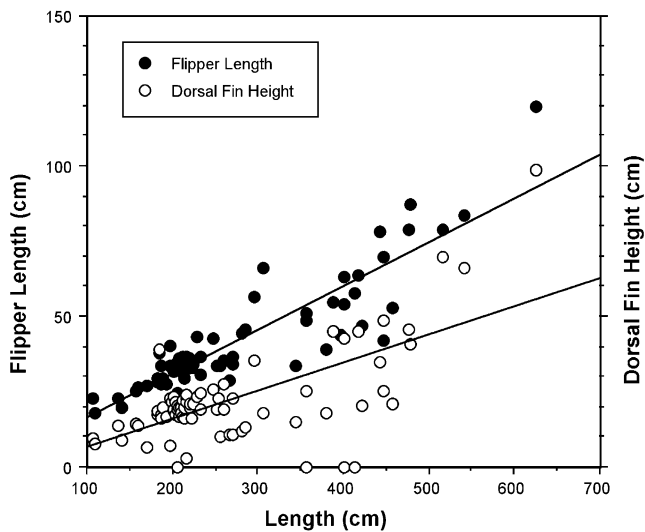


Fig. 12. Relationships between flipper length and dorsal fin height with respect to body length for odontocete whales. A total of 81 individuals were examined from 26 species. Flipper length (FL) increased with increasing body length (BL) according to the equation  $FL = 1.80 + 0.15BL$  ( $r = 0.89$ ). Dorsal fin height (DF) increased directly with BL according to the equation  $DF = -2.93 + 0.09BL$  ( $r = 0.65$ ). From [45].

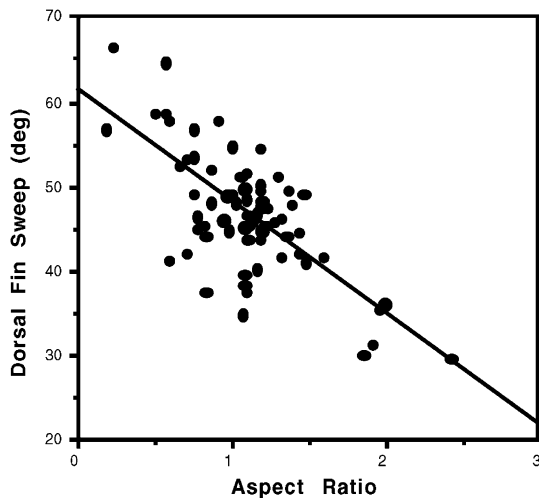


Fig. 13. Relationship of dorsal fin sweep ( $\Delta$ ) to AR from data in [45]. The regression line is described by the equation  $\Delta = 61.29 - 13.16AR$  ( $r = 0.70$ ).

between phases within a paddling cycle. The muskrat showed a 55% reduction in planar area between power and recovery phases of the feet [36].

The paddle-like foot has a shape that is circular or triangular with a constriction at the attachment point with the body. This constriction minimizes interference drag with the body [130], [131]. In some cases, the constriction displaces the center of area of the paddle further from the body and provides a longer lever arm to increase the velocity of the paddle [36], [74]. Long stroke lengths and high paddling frequencies are not efficient; it is more efficient to generate thrust by acceleration of a large fluid mass to a small velocity than a small mass to a high velocity [72]. In small semi-aquatic rodents with high paddling frequencies and small paddle areas, inertial and added mass effects account for 31%–51% of the total energy necessary for paddling

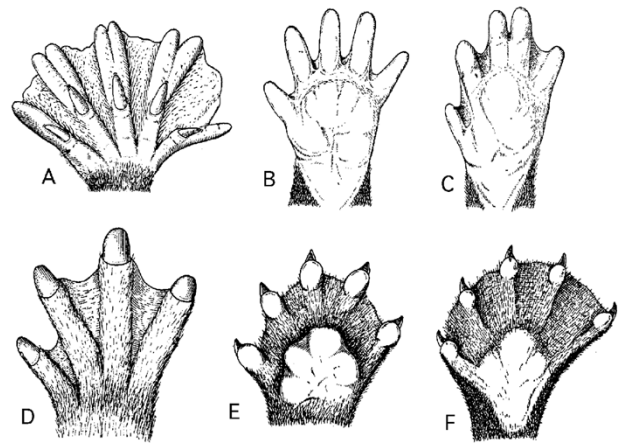


Fig. 14. Anterior feet of semi-aquatic mammals showing the range of interdigital webbing, which is used as a paddle. (A) Platypus, (B) African clawless otter, (C) Oriental small-clawed otter, (D) capybara, (E) North American river otter, and (F) spotted-necked otter are shown. From [11], with permission of the publisher.

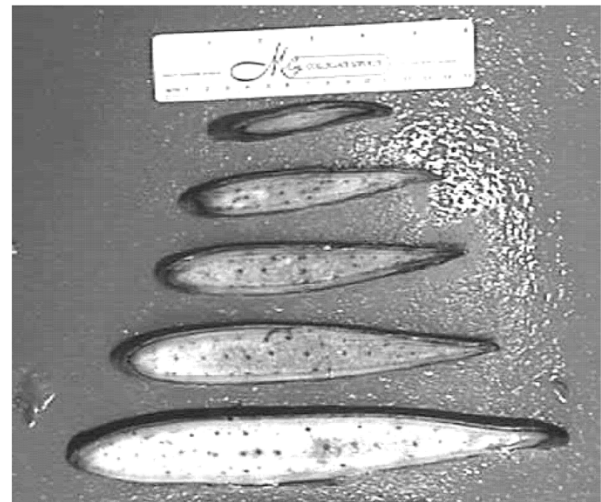


Fig. 15. Sections of dorsal fin from bottlenose dolphin (*Tursiops truncatus*). From [45].

[42]. When paddles are used for maneuvering, however, efficient force production may not be necessary. Maneuvering in animals typically requires the rapid production of destabilizing forces without consideration of efficiency or economy.

Tests on models of fish demonstrated that fins with circular and triangular planforms produced greater pressure drags than square or rectangular planforms [131]. A triangular fin shape has a greater moment of inertia than square and rectangular fins [131]. Paddles with a triangular shape can generate thrust, while reducing energy losses due to added mass and inertial effects. When swept through an arc, the distal segment of the paddle produces the majority of thrust, because it experiences the highest flow rate with a large area moment of inertia referenced to the center of rotation. Blake [74] found that 80% of the thrust and work produced was produced by the distal quarter of a triangular fin.

2) AR: The AR is calculated as the square of the span divided by the planar area [56]. In mysticetes, the AR of flippers is largest for the humpback whale *Megaptera* (AR = 6.1;

TABLE I  
SECTIONAL CHARACTERISTICS FROM MID-SPANS OF CONTROL SURFACE FINS FROM CETACEANS, SEA LIONS,  
AND PENGUINS. DATA FROM [29], [39], [125], [133], [136], [179], AND [180].

Species	Fin type	Maximum	Distance from	Leading edge	Trailing edge	Distance from		Distance from
		thickness	leading edge to	radius	thickness	leading edge to	Minimum	leading edge to
		% chord	maximum thickness	% chord	% chord	maximum camber	Cp	minimum Cp
			% chord	% chord	% chord	% chord		% chord
<i>Delphinus bairdi</i>	fluke	21.1	32	4.2	0.46	symmetrical	-0.74	15
<i>Lagenorhynchus obliquidens</i>	fin	19.3	33	3.8	0.90	symmetrical	-0.66	14
<i>Phocoenoides dalli</i>	fin	15.2	36	2.4	0.28	symmetrical	-0.46	16
<i>Phocoena phocoena</i>	fin	12.4	27.6	1.7		symmetrical		
<i>Megaptera novaeangliae</i>	flipper	20.0	33			symmetrical		
dolphins	fluke	19.0 - 24.0	24.0 - 30.0	3.2 - 7.4		symmetrical		
<i>Zalophus californianus</i>	flipper	21.3	24.4			symmetrical		
<i>Pygoscelis antarctica</i>	flipper	15.0	35	3.0		30		
<i>Pygoscelis adeliae</i>	flipper	15.0	30	4.0		50		

[125]). For odontocete flippers, AR values range from 1.9 for paddle-like flipper of *Orcinus orca* to 7.7 for the highly swept elongate flipper of *Globicephala melaena* [45]. Dorsal-fin AR is significantly smaller than the flipper AR. The largest dorsal-fin AR of 2.4 is found for a male *Orcinus orca*. For cetaceans that possess a dorsal fin, the smallest AR is displayed for the triangular fin of *Inia geoffrensis*. Dorsal fin sweep is inversely related to AR (Fig. 13) so that animals with high sweep have low AR and vice versa.

AR for penguin flippers varies from 4.2 to 4.5 [29]. Fish *et al.* [132] reported AR for two sea lions as 4.1 and 4.2. However, Feldkamp [39] reported an average AR of 7.9 for sea lion flippers, when AR was calculated as the span of the flippers divided by their chord.

3) *Cross-Sectional Design*: The cross-section design of flippers and other control surfaces displays the characteristic fusiform design (Fig. 15; [29], [40], [113], [125], [133], [134]). The addition of skeletal elements in the flippers makes these appendages relatively thick as compared to control surfaces that are composed solely of collagenous material, such as the flukes and dorsal fin of cetaceans. Flippers of penguins are cambered in cross-section [29], whereas flippers of marine mammals, such as sea lions and cetaceans, are uncambered (i.e., symmetrical about the chord line) [40], [125]. The tip of the humpback whale flipper is scooped out along the ventral surface of the leading edge, producing a concavity [125], [127].

Despite the similarity of cross-sectional designs of flippers with engineered foil sections, flippers have not been fully analyzed with the rigor demonstrated for wing sections. Available data on sectional characteristics of high-AR control surfaces from marine mammals and penguins are provided in Table I. The most typical index of shape used to describe the cross-sectional geometry of flippers is the maximum thickness as a percent of chord length (inverse of fineness ratio). At mid-span, biological control surfaces have thicknesses ranging from 15.0%

to 24.0% of chord (Table I). Maximum thickness varies along the span of flippers with lower values closer to the root. For penguins, the maximum thickness as a percent of chord length varies from 14% to 17% [29]. Sectional thickness of the sea lion (*Zalophus californianus*) flipper varies from 31.3% of chord at the root to 18.5% of chord near the tip [40]. Conversely, humpback whale flippers have high sectional thickness at the tip (27.8% of chord) with the lowest sectional thickness (20% of chord) near mid-span [125].

The distance from the leading edge of the high-AR control surface to the maximum thickness varies 24% to 36% of chord (Table I). The placement of the maximum thickness indicates a fairly even pressure distribution in the chordwise direction [133]. This morphology would potentially delay separation. In addition, the prominent leading-edge radius would prevent leading-edge separation during maneuvers with an increased angle of attack.

Camber in penguin flippers effectively increases lift. While it may be a remnant of an evolutionary pathway from flight, the wing structure can be useful in force production for propulsion and turning maneuvers.

4) *Lift and Drag Characteristics*: Well-designed control surfaces maximize the ratio of lift ( $L$ ) to drag ( $D$ ) generated by their action or passive from the ambient water flow [56], [98]. An increase in the maximum  $L/D$  with increasing size is achieved by increasing the span of the control surface more rapidly than the square root of the planar area, thereby increasing AR [82], [135], [137]. The longer span of a high-AR fluke increases the mass of water deflected posteriorly, augmenting lift. However, AR above 8–10 provides little further advantage [56], [113].

The addition of appendages increases the drag. As the pectoral flippers of sea turtles, penguins, and sea lions are used for propulsion, it is impossible to differentiate the thrust from the drag for these appendages and drag estimates have not been

performed. Many cetaceans, however, have flippers that project laterally from the body and add substantially to the total drag. The body of the harbor porpoise (*Phocoena phocoena*) makes a disproportionate contribution to the total drag in that the body is 87.6% of the total surface area, but only 64.3% of the drag [138]. The dorsal fin, pectoral flippers, and flukes comprised only 2.6%, 4.2%, and 5.6%, respectively, of the total surface area of the harbor porpoise; however, these appendages are responsible for 35.7% of the total drag (4.3%, 18.0%, and 13.4%, respectively). The drag added by the appendages of *Tursiops* was estimated as 28% of the total drag [139]. The added increase in drag due to the appendages is caused by interference drag as flow over the body is distorted by the appendages and induced drag from differential pressure in lift generation by the appendages [30], [44], [56], [88], [130]. The induced drag component is the energy lost due to tip vortices that are generated by pressure differences between the two sides of the flippers and dorsal fin during maneuvers [30], [56].

Induced drag is highly dependent on AR, with high drag associated with low AR and untapered hydrofoils [56]. Induced drag is produced as a consequence of the lift generated by the control surface. When canted at an angle to the water flow, lift is produced by deflection of the water and pressure difference between the dorsal and ventral surfaces of the control surface [43], [56], [73], [86]. The pressure difference produces spanwise cross-flows that go around the control surface tip, resulting in the formation of spiraling vortical flow. The flow is shed from the fluke tip as longitudinal tip vortices. The energy dissipated by the vortices represents the induced drag. High AR and tapering of the flippers reduces tip vorticity and induced drag [24], [56], [71].

Induced drag is also limited by sweep. van Dam [82] showed that a tapered wing with sweepback or crescent design could reduce induced drag by 8.8% as compared to a wing with an elliptical planform. Minimal induced drag is fostered by a swept-wing planform with a root chord greater than the chord at the tips, giving a triangular shape [140], [141]. This optimal shape approximates the planform of flippers [29], [45].

Sweep together with taper has the effect of concentrating the surface area toward the trailing edge. This would effectively shift the lift distribution posterior of the CG, affecting pitching equilibrium [56], [135]. The combination of low sweep with high AR (Fig. 13) can aid in lift generation for maneuvers. Highly swept-back low-AR wings produce maximum lift when operating at large angles of attack, when low-sweep high-AR designs would fail [107]. However, the maximum lift is reduced with increasing sweep angle for a given AR [142]. The relationship between sweep and AR also indicates a structural limitation to the strength and stiffness of the control surfaces [82], [143]. The ability to sustain certain loads without breaking is considered a major constraint on increasing span and AR [144].

Analysis of pressure distributions of control surfaces in dolphins was performed by Lang [133]. Using a two-dimensional (2-D) potential flow airfoil program, he calculated the pressure distribution for single sections from the dorsal fins of the Pacific striped dolphin (*Lagenorhynchus obliquidens*) and Dall's porpoise (*Phocoenoides dalli*). Their minimum pressures were located 14%–16% of chord (Table I, Fig. 16), followed by a

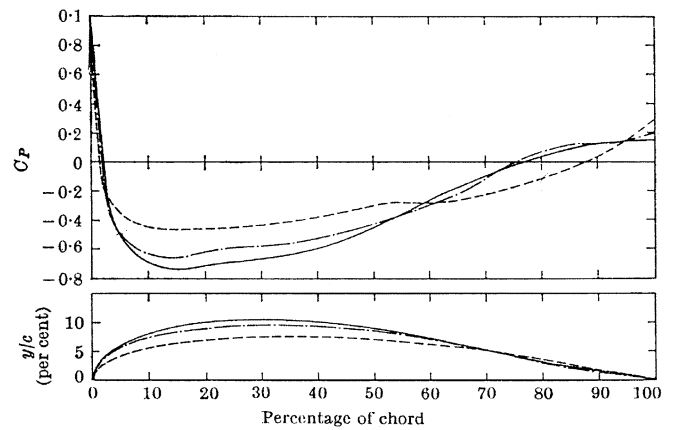


Fig. 16. (bottom) Profiles and (top) pressure distribution for sections at 50% of span for the tail fluke of the common dolphin, *Delphinus bairdi* (—); dorsal fin of the Pacific striped dolphin, *Lagenorhynchus obliquidens* (---); and dorsal fin of Dall's porpoise, *Phocoenoides dalli* (- - -). From [133] with permission of the author and publisher.

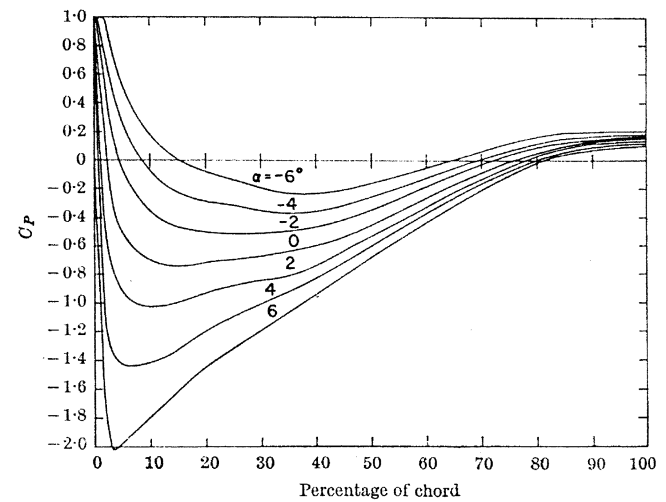


Fig. 17. Effect of angle of attack on the pressure distribution of a 2-D foil based on a section from a dolphin fluke at 50% of span. From [133] with permission of the author and publisher.

region of gentle adverse pressure gradient to 50%–60% of the chord and followed by a steep adverse pressure gradient. Lang [133] considered that the fins were ideally suited to operate at a Reynolds number of  $10^6$ . The fins normally operate at this Reynolds number. Fin sections examined by Lang [133] were considered relatively thick at 19.3% and 15.2% of chord for *Lagenorhynchus* and *Phocoenoides*, respectively. This thickness may add to the strength of the fin and may permit greater variations in the angle of attack during maneuvers. The section geometry could prevent excessive minimum pressure peaks at the leading edge and, thus, prevent flow separation and cavitation. Cavitation near the water surface was expected to occur with a zero angle of attack at 17.3–20.7 m/s [133].

Pressure distributions of the fins and flukes from dolphins (Fig. 16) were not similar to common airfoils [133]. Fin profiles were judged to be a compromise between airfoils FX05-191 and EA6(-1)-018. The favorable pressure gradient near the nose and gentle adverse gradient appeared to optimize the length of the laminar boundary layer and resist separation [133]. At angles of attack up to  $4^\circ$ , the dolphin fin should not incur separation and increased drag (Fig. 17).

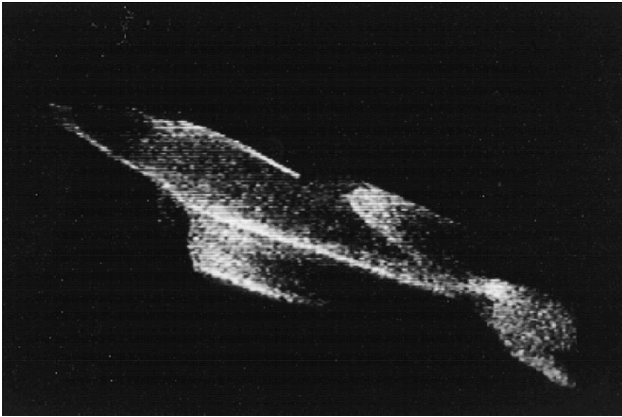


Fig. 18. Bioluminescence image of a gliding dolphin (*Tursiops truncatus*). From [149] with permission of the author.

When actively swimming, bioluminescent “contrails” frequently have been reported [145]–[147], extending from the flukes, flippers, and dorsal fins of dolphins. These contrails are the tip vortices generated from the differential pressures along the two surfaces of a lifting surface.

Flow visualization using bioluminescence within the boundary layer of a dolphin was exploited by Rohr and Latz with their colleagues [148], [149]. The bioluminescence was produced by unicellular plankton called dinoflagellates. The bioluminescence response of dinoflagellates was calibrated to a hydrodynamic-induced shear stress [148]. Stimulation of bioluminescence occurred above a shear stress of approximately 1 dynes/cm<sup>2</sup> in both laminar and turbulent flows. A gliding dolphin moving through water with the dinoflagellates was able to stimulate bioluminescence over its body (Fig. 18; [149]). There was a conspicuous lack of bioluminescence over the leading edges of the flippers and dorsal fin. During rectilinear glides, the boundary layer remained attached over the surface of the dorsal fin and flippers. Flow separation was noted at the trailing edges of these control surfaces. From Fig. 18, disturbed flow can be observed at the base of the flippers, potentially due to interference effects. Lines of bioluminescence were apparent from the tips of the dorsal fin and flippers during turning maneuvers [149]. These contrails were most likely the result of pressure differences between the sides of the control surfaces, which were associated with lift generation.

Position and number of tubercles on the humpback flipper suggest analogues with specialized leading-edge control devices associated with improvements in hydrodynamic performance. Bushnell and Moore [150] suggested that humpback tubercles may reduce drag on the flipper. The occurrence of “morphological complexities” on a hydroplane could reduce, or use, tip bleed flow to decrease drag and improve lift generation to prevent tip stall. Alternatively, various biological wings utilize leading-edge control devices to maintain lift and avoid stall at high attack angles and low speeds [151]. Hydroplanes used in turning must operate at high angles of attack while maintaining lift.

Fish and Battle [125] considered that the tubercles of the humpback whale flipper may function to generate vortices by unsteady excitation of flow to maintain lift and prevent stall at

high angles of attack. The function of the tubercles would be analogous to strakes used on aircraft. Strakes generate large vortices that change the stall characteristics of a wing [125], [130], [152], [153]. Stall is postponed because the vortices exchange momentum within the boundary layer to keep it attached over the wing surface. Lift is maintained at higher angles of attack with strakes as compared to wings without strakes, although maximum lift is not increased by strakes. Increased angle of attack is necessary during turning maneuvers to generate the lift force for the turn [91], [107], [135]. The ability to maintain lift at high angles of attack would be advantageous for humpback whales in maneuvering.

Flow visualization experiments conducted on a model wing section with leading edge tubercles similar to those on humpback flippers showed that vorticity was produced (Wallace and Smith, personal communication). Bearman and Owen [154] demonstrated that a wavy leading edge on a bluff body produced a 30% drag reduction. The wavy leading edge generates periodic variation in the von Karman wake across the span [155]. A wide wake occurs at a trough (i.e., leading-edge loops downstream) and a narrow wake occurs at a peak in the leading edge. An inviscid panel method simulation of a National Advisory Committee for Aeronautics (NACA) 63<sub>4</sub> – 021 wing with leading edge tubercles showed a 4.8% increase in lift and a 10.9% reduction in induced drag at 10° angle of attack [153].

#### IV. MANEUVERING PERFORMANCE

##### A. Cetacean Maneuvering

In general, cetaceans possess a stable morphological design (i.e., anterior position of the CG, concentration of control surfaces posterior of the CG, dihedral, and sweep of control surfaces) that enhances stability, thereby potentially constraining turning performance [62]. Compared to fishes, cetaceans have few control surfaces.

The flippers of cetaceans act to passively dampen the rate of growth of a perturbation [59]. The position of the flippers increases both the area and span of the body anterior of the center of mass. Pitching movements will produce a force normal to the planar area of the flippers that will act to resist vertical motions of the head. The increased area of the flippers increases the added mass and inertia at the anterior end of the animal, effectively dampening recoil movements [56], [110]. The vertical movements of the flippers are asynchronous with the propulsive cycle of the flukes [87]. The large phase differences between the motions of the flippers and the flukes of cetaceans help to generate resistive forces at the flippers that would counter pitching rotations generated by the vertical forces produced by the flukes. However, cetaceans with flippers of relatively large areas showed no effect with respect to decreasing dorso-ventral excursions at the rostrum [87]. One possible reason for this observations is that cetaceans do not show differences between the planar area of the flippers and the planar area of the flukes. Since the fluke area is proportional to force production, the resistive force generated from recoil at the flippers would be proportionally similar.

A dimensionless maneuverability index was used by Maslov [63] to compare the turning performance of dolphins with

submarines. The index was a compilation of variables including length, mass, turning velocity, time to execute the turn, power output, and turning radius. The results of the comparison showed that dolphins were more maneuverable than submarines (*USS Albacore* and *USS Skipjack*). Length-specific turning radii for a common dolphin and bottlenose dolphin ranged from 0.5 to 1  $L$ . Maslov [63] and Aleyev [59] considered that dolphins turned most effectively around the pitch axis, because of the orientation of the flippers and flukes. Within the horizontal plane, dolphins were considered to be more stable.

Fish [62], [101] examined the horizontal turning performance of various cetaceans, including the bottlenose dolphin (*Tursiops truncatus*), killer whale (*Orcinus orca*), Commerson's dolphin (*Cephalorhynchus commersonii*), Pacific white-sided dolphin (*Lagenorhynchus obliquidens*), false killer whale (*Pseudorca crassidens*), beluga (*Delphinapterus leucas*), and Amazon river dolphin (*Inia geoffrensis*). *Orcinus* was the largest cetacean with one individual of 4536 kg, whereas the smallest, at 29 kg, was *Cephalorhynchus*. *Pseudorca* and *Lagenorhynchus* were generally regarded as fast swimmers, whereas *Delphinapterus* and *Inia* are considered to be slow swimmers [45]. *Delphinapterus* and *Inia* are different from the other cetaceans by possessing mobile necks and flippers. *Inia* is capable of a notable degree of lateral flexion. In addition, the dorsal fin is reduced in *Inia* and absent in *Delphinapterus*.

Cetaceans executing yawing turns showed two turning patterns: powered and unpowered [62], [101]. Powered turns were defined as turns in which the animal was continuously propelling itself by the dorso-ventral oscillations of the flukes, whereas, in unpowered turns, the animal glided through the turn without apparent use of the caudal propulsor. Turns were initiated from the anterior of the animal with lateral flexion of the head and rotation of the flippers into the turn. The flippers also were adducted. During unpowered turns, substantial lateral flexion of the peduncle was observed in addition to twisting at the base of the flukes. At the beginning of a turn, *Tursiops* will twist the inside fluke blade downward by  $15^{\circ}$ – $45^{\circ}$  from the horizontal, before reversing the rotation of the flukes by  $58^{\circ}$ – $88^{\circ}$  as the animal exits the turn [62]. *Pseudorca* flexes its body during the turn and only twists its flukes at the end of the turn by  $18^{\circ}$ – $53^{\circ}$  with the outside fluke blade depressed. The twisting action allows the animal to use the flukes in conjunction with the peduncle as a rudder. This action is only possible in unpowered turns because the control surfaces are uncoupled from propulsion, permitting increased flexibility of the spine [62]. Inward banking occurs during unpowered turns. Rolling oscillations around the longitudinal axis occurred during powered turns that were associated with propulsive fluke motions.

Both *Inia* and *Delphinapterus* proved to be exceptions to the general cetacean turning pattern [62], [101]. *Inia* showed no tendency to bank during turns and used its flexible body to produce the turn. Without a dorsal fin, *Delphinapterus* would bank  $90^{\circ}$  with its ventral surface facing into the turn. This action allowed it to use a greater surface area and provided greater body flexion to effect the turn. High bank angles also are displayed by penquins and sea lions, which lack a dorsal fin [46], [156].

The force necessary to maintain a curved trajectory of a given radius is directly related to the square of the velocity and the

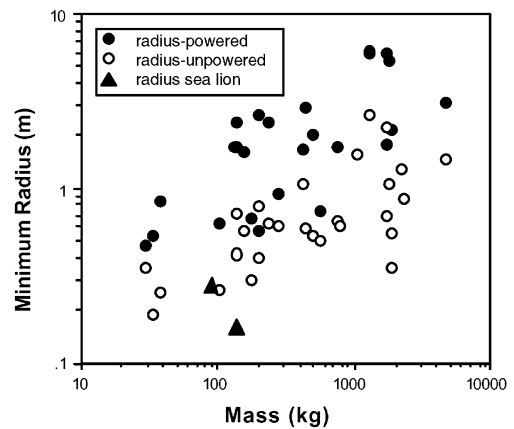


Fig. 19. Minimum turning radius plotted against body mass for individuals from Fish [101]. Circles represent cetaceans for powered (solid) and unpowered (open) turns and triangles represent unpowered turns by sea lions (*Zalophus californianus*).

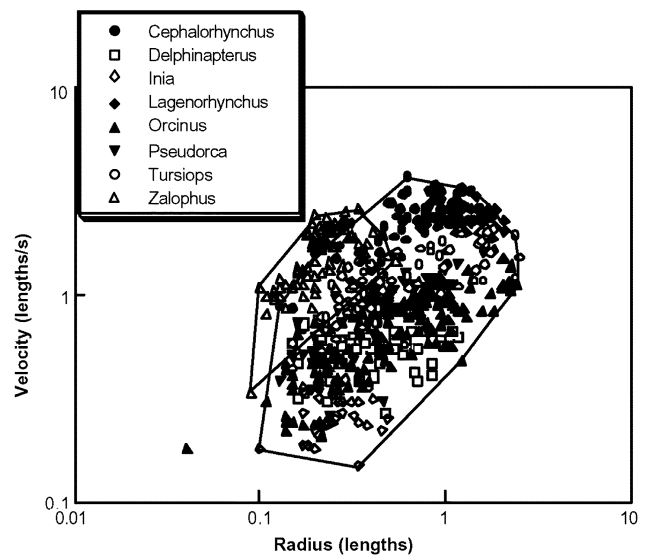


Fig. 20. Average length-specific velocity in relation to length-specific turning radius. Polygons are drawn around data for cetaceans and around data for *Zalophus*. The single point outside the cetacean polygon represents a 1725.2-kg 5.05-m *Orcinus* that was able to produce a turn radius of 4% of body length by ventrally flexing the posterior half of the body. The flukes were used to pivot the animal around its longitudinal axis.

mass of the body [157], [158]. Minimum turning radius plotted for cetaceans was associated with body mass (Fig. 19). Unpowered turns for cetaceans had smaller minimum radii than powered turns for the same individuals [62]. Cetaceans generally demonstrated minimum unpowered turning radii of  $<0.5L$  (Fig. 19). Minimum radii within each species ranged from 0.11 to 0.17  $L$ . A 5-m-long *Orcinus* was able to turn within 0.4  $L$  [101]. The turn was performed by depressing the posterior half of the body and rotating around the vertically oriented tail. Although the turning radius was small, the speed was low (0.93 m/s) due to the extra drag produced from the body orientation.

Different levels of performance between species were indicated when all the data for turning radius were plotted as a function of velocity (Fig. 20). *Inia* and *Delphinapterus* produced low-speed small-radius turns. Faster speed but larger radius turns were performed by *Lagenorhynchus* and

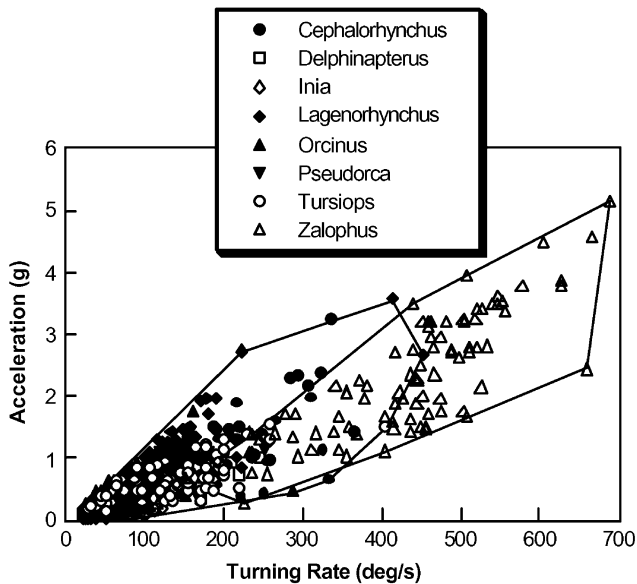


Fig. 21. Relationship between centripetal acceleration and turning rate. Polygons are drawn around data for cetaceans and around data for *Zalophus*.

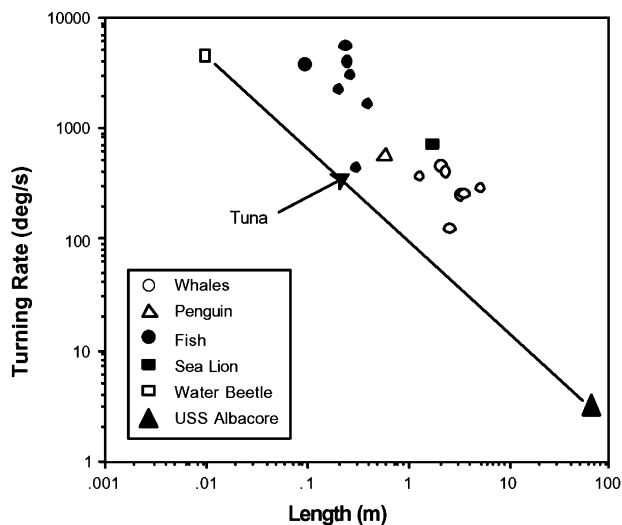


Fig. 22. Turning rate as a function of body length. Data from [95], [101], [156], and [163]–[165].

*Cephalorhynchus* and intermediate performance was displayed by *Orcinus*, *Pseudorca*, and *Tursiops*.

Turning performance is illustrated in Fig. 21 by a plot of centripetal acceleration and turning rate. Most data for cetaceans are clustered at accelerations  $<1.5g$  with turning rates  $<200^\circ/s$ . Some dolphins were able to exceed these lower values for cetaceans with *Lagenorhynchus* displaying the maximum performance with an acceleration of  $3.6g$  and turning rate of  $453^\circ/s$  during unpowered turns. Other cetaceans exhibited lower performance. The lowest centripetal accelerations occurred in *Inia* followed by *Delphinapterus*, which both swam slowly. Although higher than underwater vehicles (Fig. 22; [63], [104], [105]), turning rates were lower than exhibited by fish, penguins, and sea lions [95], [101], [104], [105], [156], [159].

Flexible bodies and mobile control surfaces provide mechanisms to induce instabilities for turning maneuvers. Cetaceans

with more flexible body designs (e.g., *Inia* and *Delphinapterus*) sacrifice speed for maneuverability, whereas species with more restricted flexibility (e.g., *Lagenorhynchus* and *Cephalorhynchus*) produce faster, but wider turns [101], [160]. As morphological differences can be correlated with behavioral differences [161], features that affect the stability and maneuverability of cetaceans appear to be associated with their prey type and habitats.

*Inia* inhabits rivers, lakes, and floodplain forests and grasslands. These habitats are structurally complex, where decreased turn radius and precise slow maneuverability would be necessary. Similarly, the distribution of *Delphinapterus* is in complex environments including shallow waters, coastal habitats, rivers, and pack ice. *Delphinapterus* feeds on less mobile prey such as bottom organisms and large zooplankton [160]. The more stable design of fast swimming cetaceans may limit these animals to locomoting and foraging in pelagic habitats.

The ability to roll permits cetaceans to reorient their body to take advantage of the increased flexibility by ventral flexing of the bodies. Aerial views of foraging dolphins (*Tursiops truncatus*) showed that the animals rolled  $90^\circ$  during the final lunge for fish [162]. Bending of the body allowed the tip of the rostrum to turn at a rate of up to  $1370^\circ/s$  with a radius of 0.08 body lengths.

A remarkable maneuver undertaken by spinner dolphins (*Stenella longirostris*) is to leap out of the water and rapidly spin around its longitudinal axis [166]. Although the preparatory movements prior to the leap have not been observed, the dolphin has to start spinning before it leaves the water. Underwater video of Pacific striped dolphins (*Lagenorhynchus obliquidens*) spinning while swimming horizontally shows that the dolphin spins by using its flippers to provide the force to rotate its body (personal observations).

### B. Sea Lion Maneuvering

Compared to cetaceans, the placement of control surfaces, mechanisms of propulsion, and body configuration indicate greater instability and, thus, maneuverability by California sea lions (*Zalophus californianus*). The control surfaces of *Zalophus* are represented by pectoral and pelvic flippers [46], [119]. The roots of the larger pectoral flippers are located near the CG [101]. This placement of the pectoral flippers is dynamically unstable. The flippers provide little rotational dampening about the yaw and pitch axes, although they could retard rotational and translational motion in regard to roll and heave, respectively. The smaller pelvic flippers are in the preferred location to develop sufficient torque to act like an airplane stabilizer or ship rudder and resist rotational instabilities.

The attitude of the *Zalophus* control surfaces are highly variable because of the high mobility of the pectoral and pelvic flippers [46], [119]. Both the sweep and dihedral can be changed. The ability of the sea lion to adduct the pectoral flippers against the body and adduct the pelvic flippers can effectively produce a condition in which the animal is devoid of control surfaces and potentially susceptible to all instabilities. The mobility of the pectoral and pelvic flippers also permits dynamic production of lift that can induce torques around the CG to promote instabilities. The location of the pectoral flippers close to the CG would not produce large torques and would be less effective in rapidly



Fig. 23. Demonstration of body flexibility by the California sea lion.

inducing turns. The large projected area of the flippers may help compensate for the reduced torque. However, the pectoral flippers are used for propulsion [11], [39], [40], and propulsors arranged around CG are postulated to promote maneuverability [100].

The body of *Zalophus* is highly flexible (Fig. 23). Bending of the body and neck is an integral component of turning in conjunction with the flippers of pinnipeds [46], [59]. The extremely pliable neck and body permit a sea lion to bend over backward reaching its pelvic flippers [167]. This dorsal bending was the preferred bending direction used by sea lions during turns [46]. Dorsal bending of the spine allows the body to curve smoothly, maintaining a streamlined appearance throughout a turn. As the turn is unpowered, a streamlined body will minimize drag and limit deceleration as direction changes.

Sea lions use only unpowered turns [101]. As described in [46], [53], [101], [119], and [168], the anterior end of the animal initiates the turn as the sea lion rolls  $90^\circ$  so that the ventral (abdominal) surface faces the outside of the turn and the body is flexed dorsally. The fore and hind flippers are abducted and held in the vertical plane. This maneuver brings the full area of the flippers into use. In addition, the position of the fore flippers is set to execute a power stroke and to accelerate the sea lion as it comes out of the turn.

Sea lions were able to make small radius turns while at high speed (up to 4.5 m/s). Minimum unpowered turn radii for *Zalophus* ranged from 0.9 to 0.16  $L$  [101]. While the length-specific radii were small, they were not substantially different from similar values for cetaceans (Fig. 19). However, *Zalophus* typically demonstrated smaller turn radii at higher speeds than cetaceans (Fig. 20). In addition, turning rates were higher for *Zalophus*, exceeding the maximal performance of cetaceans (Fig. 21). Sea lions are able to execute turns of  $5.13 g$  at  $690^\circ/s$ . This performance exceeds the acceleration experienced during liftoff on a space shuttle [101].

Similarities have been made between the turning maneuvers of sea lions and the banking turns displayed by birds and airplanes [53]. In these latter banking turns, the wings generate lift that is resolved into vertical and horizontal vector components. The vertical component counters the gravitational force and keeps the aircraft from losing altitude. The horizontal vector is directed toward the center of rotation and provides the centripetal force necessary for the turn.

As sea lions swim in an environment with a density similar to their body composition, these animals can be near neutrally buoyant, negating the necessity of a vertical component during turns in the horizontal plane. Thus, the sea lion can bank  $90^\circ$  without changing depth. The horizontally directed lift from the flippers would produce centripetal force necessary for the turning maneuver. While the pectoral flippers can be rotated to produce an angle of attack (i.e., angle between the flipper chord and the incident flow), bending of the spine would aid in orientation of the flippers for lift generation. However, there is no direct evidence that the flippers are canted at an angle of attack to effect a turn. Indeed, the location of the flippers close to CG reduces the torque to produce the turn. The pectoral flippers are particularly important in generating the lift necessary to roll the body. Other surfaces used to control the turn are the head and pelvic flippers. The head leads the turn and determines direction. The pelvic flippers act as stabilizers to prevent the posterior portion of the body from deviating from the curved trajectory of the turn [46].

### C. Humpback Whale Maneuvering

The humpback whale (*Megaptera novaeangliae*) is the most acrobatic of the baleen whales. Its elongate wing-like flippers are important in its ability to maneuver. Observations of swimming performance by humpback whales show them to be highly maneuverable [127], [169], using their extremely mobile flippers for banking and turning [60], [170]. This maneuverability is particularly associated with the feeding behavior of humpback whales. These whales feed on patches of plankton or fish schools, including euphausiids, herring, and capelin [124], [171], [172]. Turning is widely used in feeding employed with lunging and bubbling behaviors [173].

In lunge feeding, whales rush (approximately 2.6 m/s) toward their prey from below while swimming up to the water surface at a  $30^\circ$ – $90^\circ$  angle [124], [173]. In “inside loop” behavior, the whale swims away rapidly from the prey aggregate with its flippers abducted and protracted [60], then rolls  $180^\circ$ , making a sharp U turn (“inside loop”) and lunges toward the prey [173]. The entire “inside loop” maneuver is executed in 1.5–2 body lengths of the whale. Rapid turning maneuvers are required also for “flick feeding,” which is performed in approximately 3 s [124]. In this feeding behavior, the whale dives until the base of the flukes is at the water surface and the tail is flicked forward, producing a wave. The whale surfaces with its mouth open into the wave.

In “bubbling” behaviors, underwater exhalations from the blowhole produce bubble clouds or columns that concentrate the prey [171], [174]. Columns of bubbles arranged as rows, semicircles, and complete circles form “bubble nets” [124], [173]. Bubble nets are produced as the whale swims toward the surface in a circular pattern from a depth of 3–5 m. At completion of the bubble net, the whale pivots with its flippers and then banks to the inside as it turns sharply into and through the center of the net [173], [175]. Bubble net size varies from a minimum diameter of 1.5 m for corralling euphausiids to a maximum diameter of 50 m to capture herring [124].

Fish and Battle [125] computed the turning radius for a 9-m humpback whale. Their computations were based on the whale using the flippers to generate a centripetal force for

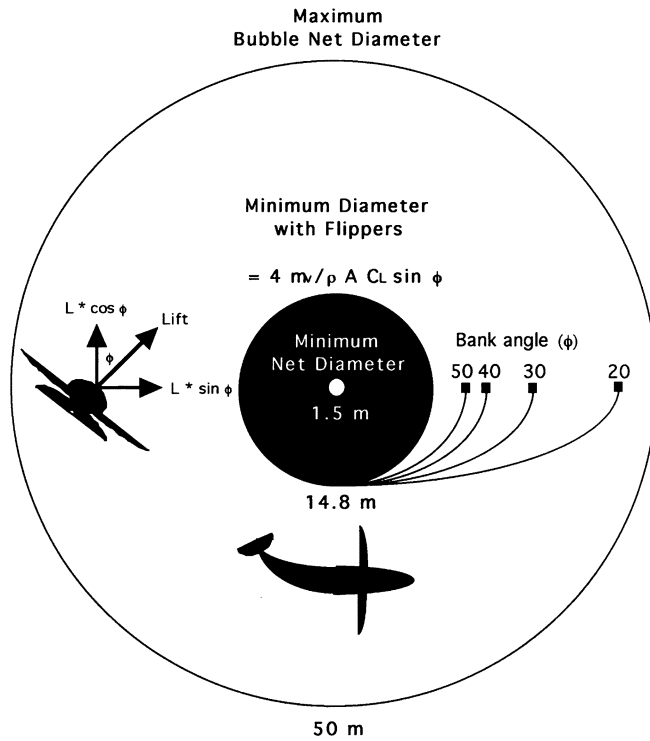


Fig. 24. Calculated and observed turning performance of the humpback whale (*Megaptera novaeangliae*). The calculated minimum turning diameter (14.8 m) for a 9-m whale is shown by the outer margin of the black circle, based on the equation shown. The margins of the turn for various bank angles are shown by curved lines. The minimum and maximum diameters of bubble nets are shown by the margin of the central white circle and the outer white circle, respectively. The lift ( $L$ ) vectors with respect to bank angle are illustrated in the inset. The silhouette indicates the dimensions of the whale.

the turn. The whale's minimum turning radius equaled 7.4 m when the banking angle ( $\phi$ ) equaled  $90^\circ$  (Fig. 24). The calculated minimum turning radius fell within the minimum and maximum radii for turns during bubbling behaviors [124]. Maximum bubble net radius (25 m) may be achieved by the humpback whale with a banking angle of  $17^\circ$ . Considering that other surfaces of the whale (e.g., flukes, peduncle, and body) are employed in turns [60], the actual minimum turning radius was assumed to be smaller [125]. Fluke span is 27%–38% of total body length [126], [127]. The relatively large size of the flukes contributes to maneuverability by increasing the lift force. However, the restricted range of motion of the flukes and body in conjunction with their use in thrust production limits their effectiveness to control maneuverability during powered swimming.

#### D. Penguin Maneuvering

Hui [156] examined the maneuvering performance of swimming Humboldt penguins (*Spheniscus humboldti*). He observed that the birds used a variety of body structures to produce turns. The steering structures included laterally compressed tail and hind feet (100% of turns analyzed), laterally compressed beak (95% of turns analyzed), and wings (35% of turns analyzed). Wings were used when maximum power for the turn was required. Turn radii of the sharpest turns averaged 0.14 m, which was 0.24  $L$ . These turns had a mean length-specific speed of 2.22

$L/s$ . Turning rate for the penguins ranged from 57.9 to 545.8 $^\circ/s$ , with a mean turning rate of 232 $^\circ/s$ .

#### E. Cephalopod Maneuvering

Turning rates by squid are considered slow at 2 s to execute a  $180^\circ$  turn [67]. Squids, which keep the mantle stiff, cannot produce turns of less than 0.5  $L$  [67]. Squids show considerable lateral side-slip when undergoing body rotation [67]. The shelled *Nautilus* can at best negotiate a turn of 2  $L$  [176], which is equivalent to submarines with inflexible hulls and turning radii of 2–3  $L$  [63].

#### F. Sea Turtle Maneuvering

Sea turtles can turn by either forelimb movements alone or by a combination of forelimb and hindlimb movements [116]. Asynchronous movements of the forelimbs of sea turtles are used to turn [8]. The duration of the flapping movements in leatherback sea turtles are shorter for the forelimb on the inside of the turn. In hatchling loggerhead turtles, both forelimb and hindlimbs are used for turning [6], [177]. The broad hindlimbs of sea turtles act as rudders [116], [178]. The lack of fusion of the ankle bones has been assumed to aid in fine adjustment of the rudder [178].

## V. CONCLUSION

The large array of biological control surfaces for nonpiscine vertebrates and cephalopods can be divided into two fundamental structures: paddles and wing-like flippers. For paddles, the major force generated is drag whereas, for the flippers, the major force is lift. To effectively generate drag, paddles have a relatively flat cross-section with a broad low-AR planform and narrow articulated base. Flippers, also including cetacean flukes and dorsal fins, have a relatively high AR and foil-like cross-section. The cross-sectional geometry suggests the ability to enhance lift production with low drag and delayed stall at high angles of attack. Performance data show that wing-like flippers are used in small radius turns at high rates. Drag-based paddles would be effective in maneuvering at low speeds in confined spaces. The basic design features of many of nonpiscine control surfaces would be easy to copy and integrate into biorobots. The use of such biological inspiration for engineered machines may aid in enhanced performance, exceeding current mechanical technology.

## REFERENCES

- [1] J. M. Gal and R. W. Blake, "Biomechanics of frog swimming. I. Estimation of the propulsive force generated by *Hymenochirus boettgeri*," *J. Exp. Biol.*, vol. 138, pp. 399–411, 1988a.
- [2] —, "Biomechanics of frog swimming. II. Mechanics of the limb-beat cycle in *Hymenochirus boettgeri*," *J. Exp. Biol.*, vol. 138, pp. 413–429, 1988b.
- [3] G. R. Zug, "Buoyancy, locomotion, morphology of the pelvic girdle and hindlimbs, and systematics of cryptodiran turtles," *Misc. Publ. Mus. Zool. Univ. Mich.*, vol. 142, pp. 1–98, 1971.
- [4] P. S. G. Stein, "Swimming movements elicited by electrical stimulation of the turtle spinal cord: The high spinal preparation," *J. Comp. Physiol.*, vol. 124, pp. 203–210, 1978.
- [5] W. F. Walker Jr., "Swimming in sea turtles of the family cheloniidae," *Copeia*, vol. 1971, pp. 229–233, 1971.

- [6] J. Davenport and W. Clough, "Swimming and diving in young loggerhead sea turtles (*Caretta caretta L.*)," *Copeia*, vol. 1986, pp. 53–57, 1986.
- [7] J. Davenport, "Locomotion in hatchling leatherback turtles *Dermochelys coriacea*," *J. Zool., Lond.*, vol. 212, pp. 85–101, 1987.
- [8] S. Renous and V. Bels, "Comparison between aquatic and terrestrial locomotions of the leatherback sea turtle (*Dermochelys coriacea*)," *J. Zool., Lond.*, vol. 230, pp. 357–378, 1993.
- [9] J. A. Massare, "Swimming capabilities of Mesozoic marine reptiles: Implications for method of predation," *Paleobiol.*, vol. 14, pp. 187–205, 1988.
- [10] —, "Swimming capabilities of mesozoic marine reptiles: A review," in *Mechanics and Physiology of Animal Swimming*, Q. Bone, L. Maddock, and J. M. V. Rayner, Eds. Cambridge, MA: Cambridge Univ. Press, 1994, pp. 133–149.
- [11] A. B. Howell, *Aquatic Mammals*. Springfield, IL: Charles C. Thomas, 1930.
- [12] J. Lighthill, "Hydrodynamics of aquatic animal propulsion—A survey," *Ann. Rev. Fluid Mech.*, vol. 1, pp. 413–446, 1969.
- [13] M. Taylor, "Reptiles that took on the sea," *New Sci.*, vol. 26, pp. 48–51, 1987.
- [14] R. Motani, "Scaling effects in caudal fin propulsion and the speed of ichthyosaurs," *Nature*, vol. 415, pp. 309–312, 2002.
- [15] —, "Swimming speed estimation of extinct marine reptiles: Energetic approach revisited," *Paleobiol.*, vol. 28, pp. 251–262, 2002.
- [16] R. C. Osburn, "Adaptive modifications of the limb skeleton in aquatic reptiles and mammals," *Ann. N.Y. Acad. Sci.*, vol. 16, pp. 447–482, 1906.
- [17] J. A. Robinson, "The locomotion of plesiosaurs," *N. Jb. Geol. Paläont., Abh.*, vol. 149, pp. 286–332, 1975.
- [18] S. Tarsitano and J. Riess, "Plesiosaur locomotion—Underwater flight versus rowing," *N. Jb. Geol. Paläont., Abh.*, vol. 164, pp. 188–192, 1982.
- [19] S. J. Godfrey, "Plesiosaur subaqueous locomotion a reappraisal," *N. Jb. Geol. Paläont., Mh.*, vol. 11, pp. 661–672, 1984.
- [20] J. Riess, "Fortbewegungsweise, Schwimmphysik, und Phylogenie der Ichthyosaurier," *Palaeontographica A*, vol. 192, pp. 93–155, 1986.
- [21] R. V. Baudinette and P. Gill, "The energetics of 'flying' and 'paddling' in water: Locomotion in penguins and ducks," *J. Comp. Physiol. B*, vol. 155, pp. 373–380, 1985.
- [22] T. L. Aigeldinger and F. E. Fish, "Hydroplaning by ducklings: Overcoming limitations to swimming at the water surface," *J. Exp. Biol.*, vol. 198, pp. 1567–1574, 1995.
- [23] F. E. Fish, "Kinematics of ducklings swimming in formation: Energetic consequences of position," *J. Exp. Zool.*, vol. 272, pp. 1–11, 1995.
- [24] J. M. V. Rayner, "Vorticity and propulsion mechanics in swimming and flying animals," in *Konstruktionsprinzipien lebender und ausgestorbener Reptilien*, J. Riess and E. Frey, Eds. Tubingen, Germany: Univ. Tubingen, 1985, pp. 89–118.
- [25] B. D. Clark and W. Bemis, "Kinematics of swimming of penguins at the detroit zoo," *J. Zool., Lond.*, vol. 188, pp. 411–428, 1979.
- [26] C. A. Hui, "Penguin swimming. I. Hydrodynamics," *Physiol. Zool.*, vol. 61, pp. 333–343, 1988.
- [27] —, "Penguin swimming. II. Energetics and behavior," *Physiol. Zool.*, vol. 61, pp. 344–350, 1988.
- [28] R. Bannasch, "Functional anatomy of the 'flight' apparatus in penguins," in *Mechanics and Physiology of Animal Swimming*, Q. Bone, L. Maddock, and J. M. V. Rayner, Eds. Cambridge, MA: Cambridge Univ. Press, 1994, pp. 163–192.
- [29] —, "Hydrodynamics of penguins—An experimental approach," in *The Penguins: Ecology and Management*, P. Dann, I. Norman, and P. Reilly, Eds. Norton, Australia: Surrey Beatty, 1995, pp. 141–176.
- [30] F. E. Fish, "Influence of hydrodynamic design and propulsive mode on mammalian swimming energetics," *Aust. J. Zool.*, vol. 42, pp. 79–101, 1993.
- [31] A. B. Crowther, "On some points of interest connected with the platypus," in *Pap. Proc. R. Soc. Tas.*, 1879, pp. 96–99.
- [32] H. Burrell, *The Platypus*. Sydney, Australia: Angus & Robertson, 1927.
- [33] J. D. Mizelle, "Swimming of the muskrat," *J. Mamm.*, vol. 16, pp. 22–25, 1935.
- [34] A. B. Howell, "The swimming mechanism of the platypus," *J. Mamm.*, vol. 18, pp. 217–222, 1937.
- [35] T. M. Williams, "Locomotion in the North American mink, a semi-aquatic mammal. I. Swimming energetics and body drag," *J. Exp. Biol.*, vol. 103, pp. 155–168, 1983.
- [36] F. E. Fish, "Mechanics, power output, and efficiency of the swimming muskrat (*Ondatra zibethicus*)," *J. Exp. Biol.*, vol. 110, pp. 183–201, 1984.
- [37] F. E. Fish, R. V. Baudinette, P. B. Frappell, and M. P. Sarre, "Energetics of swimming by the platypus *Ornithorhynchus anatinus*: Metabolic effort associated with rowing," *J. Exp. Biol.*, vol. 200, pp. 2647–2652, 1997.
- [38] F. E. Fish, "Association of propulsive swimming mode with behavior in river otters (*Lutra canadensis*)," *J. Mamm.*, vol. 75, pp. 989–997, 1994.
- [39] S. D. Feldkamp, "Swimming in the California sea lion: Morphometrics, drag, and energetics," *J. Exp. Biol.*, vol. 131, pp. 117–135, 1987.
- [40] —, "Foreflipper propulsion in the California sea lion," *Zalophus Californianus. J. Zool., Lond.*, vol. 212, pp. 43–57, 1987.
- [41] F. E. Fish, S. Innes, and K. Ronald, "Kinematics and estimated thrust production of swimming harp and ringed seals," *J. Exp. Biol.*, vol. 137, pp. 157–173, 1988.
- [42] F. E. Fish, "Transitions from drag-based to lift-based propulsion in mammalian swimming," *Amer. Zool.*, vol. 36, pp. 628–641, 1996.
- [43] —, "Imaginative solutions by marine organisms for drag reduction," presented at the Int. Symp. Seawater Drag Reduction, J. C. S. Meng, Ed., Newport, RI, 1998, pp. 443–450.
- [44] —, "Biomechanical perspective on the origin of cetacean flukes," in *The Emergence of Whales: Evolutionary Patterns in the Origin of Cetacea*, J. G. M. MT, Ed. New York: Plenum, 1998, pp. 303–324.
- [45] F. E. Fish and J. Rohr, "Review of dolphin hydrodynamics and swimming performance," SPAWARS Syst. Center Tech. Rep. 1801, San Diego, CA, 1999.
- [46] S. J. Godfrey, "Additional observations of subaqueous locomotion in the California sea lion (*Zalophus californianus*)," *Aqu. Mamm.*, vol. 11, pp. 53–57, 1985.
- [47] D. A. Parry, "Anatomical basis of swimming in whales," *Proc. Zool. Soc. Lond.*, vol. 119, pp. 49–60, 1949.
- [48] D. S. Hartman, "Ecology and behavior of the manatee (*Trichechus manatus*) in Florida," *Spec. Publ. Amer. Soc. Mamm.*, no. 5, pp. 1–153, 1979.
- [49] T. G. Lang and D. A. Daybell, "Porpoise performance tests in a seawater tank," *Nav. Ord. Test Sta. Tech. Rep.*, 1963. 3063.
- [50] *Handbook of Marine Mammals*, vol. 3, S. H. Ridgway and R. Harrison, Eds., Academic, London, U.K., 1985, pp. 1–31. M. Nishiwaki, H. Marsh, Dugong—Dugong Dugon (Muller, 1776).
- [51] J. Videler and P. Kamermans, "Differences between upstroke and downstroke in swimming dolphins," *J. Exp. Biol.*, vol. 119, pp. 265–274, 1985.
- [52] K. M. Backhouse, "Locomotion of seals with particular reference to the forelimb," in *Symp. Zool. Soc. Lond.*, vol. 5, 1961, pp. 59–75.
- [53] G. C. Ray, "Locomotion in pinnipeds," *Nat. Hist.*, vol. 72, pp. 10–21, 1963.
- [54] F. J. Tarasoff, A. Bisailon, J. Pierard, and A. P. Whitt, "Locomotory patterns and external morphology of the river otter, sea otter, and harp seal (Mammalia)," *Can. J. Zool.*, vol. 50, pp. 915–929, 1972.
- [55] K. R. Gordon, "Locomotor behavior of the walrus (*Odobenus*)," *J. Zool., Lond.*, vol. 195, pp. 349–367, 1981.
- [56] P. W. Webb, "Hydrodynamics and energetics of fish propulsion," *Bull. Fish. Res. Bd. Can.*, vol. 190, pp. 1–158, 1975.
- [57] C. C. Lindsey, "Form, function, and locomotory habits in fish," in *Fish Physiology: Locomotion*, W. S. Hoar and D. J. Randall, Eds. New York: Academic, 1978, vol. 7, pp. 1–100.
- [58] G. J. D. Smith, K. W. Browne, and D. E. Gaskin, "Functional myology of the harbour porpoise, *Phocoena phocoena*(L.)," *Can. J. Zool.*, vol. 54, pp. 716–729, 1976.
- [59] Y. G. Aleyev, *Nekton*. The Hague, The Netherlands: Junk, 1977.
- [60] R. K. Edell and H. E. Winn, "Observations on underwater locomotion and flipper movement of the humpback whale *Megaptera novaeangliae*," *Mar. Biol.*, vol. 48, pp. 279–287, 1978.
- [61] M. Klima, H. A. Oelschläger, and D. Wunsch, "Morphology of the pectoral girdle in the amazon dolphin *Inia geoffrensis* with special reference to the shoulder joint and the movements of the flippers," *Z. Säugetierkunde*, vol. 45, pp. 288–309, 1987.
- [62] F. E. Fish, "Balancing requirements for stability and maneuverability in cetaceans," *Integ. Comp. Biol.*, vol. 42, pp. 85–93, 2002.
- [63] N. K. Maslov, "Maneuverability and controllability of dolphins," *Bionika*, vol. 4, pp. 46–50, 1970. translated from Russian.
- [64] F. E. Fish, "Swimming mode changes associated with terrestrial-semi-aquatic transition in mammals," *Amer. Zool.*, vol. 27, p. 86A, 1987.
- [65] D. P. Domning and V. de Buffrenil, "Hydrostasis in the sirenia: Quantitative data and functional interpretation," *Mar. Mamm. Sci.*, vol. 7, pp. 331–368, 1991.
- [66] R. K. O'Dor, "Limitations on locomotor performance in squid," *J. Appl. Physiol.*, vol. 64, pp. 128–134, 1988.
- [67] T. P. Foyle and R. K. O'Dor, "Predatory strategies of squid (*Illex illecebrosus*) attacking small and large fish," *Mar. Behav. Physiol.*, vol. 13, pp. 155–168, 1988.

- [68] A. Azuma, *The Biokinetics of Flying and Swimming*. Tokyo, Japan: Springer-Verlag, 1992.
- [69] P. W. Webb and R. W. Blake, "Swimming," in *Functional Vertebrate Morphology*, M. Hildebrand, D. M. Bramble, K. F. Liem, and D. B. Wake, Eds. Cambridge, MA: Harvard Univ. Press, 1985, pp. 110–128.
- [70] P. W. Webb, "Simple physical principles and vertebrate aquatic locomotion," *Amer. Zool.*, vol. 28, pp. 709–725, 1988.
- [71] T. Daniel, C. Jordan, and D. Grunbaum, "Hydromechanics of swimming," in *Advances in Comparative & Environmental Physiology 11: Mechanics of Animal Locomotion*, R. McN. Alexander, Ed. Berlin, Germany: Springer-Verlag, 1992, pp. 17–49.
- [72] R. McN. Alexander, "The history of fish mechanics," *Fish Biomechanics*, pp. 1–35, 1983.
- [73] R. W. Blake, *Fish Locomotion*. Cambridge, MA: Cambridge Univ. Press, 1983.
- [74] R. W. Blake, "The mechanics of labriform locomotion. I. Labriform locomotion in the angelfish (*Pterophyllum eimekei*): An analysis of the power stroke," *J. Exp. Biol.*, vol. 82, pp. 255–271, 1979.
- [75] T. L. Daniel, "Unsteady aspects of aquatic locomotion," *Amer. Zool.*, vol. 24, pp. 121–134, 1984.
- [76] T. L. Daniel and P. W. Webb, "Physics, design, and locomotor performance," in *Comparative Physiology: Life in Water and on Land*, P. Dejours, L. Bolis, C. R. Taylor, and E. R. Weibel, Eds. New York: Springer-Verlag, 1987, pp. 343–369.
- [77] V. I. Arreola and M. W. Westneat, "Mechanics of propulsion by multiple fins: Kinematics of aquatic locomotion in the burrfish (*Chilomycterus schoepfi*)," *J. Exp. Biol.*, vol. 263, pp. 1689–1696, 1996.
- [78] J. Lighthill, *Mathematical Biofluidynamics*. Philadelphia, PA: SIAM, 1975.
- [79] P. W. Webb, "Hydrodynamics: Nonscombrid fish," in *Fish Physiology: Locomotion*, W. S. Hoar and D. J. Randall, Eds. New York: Academic, 1978, vol. VII, pp. 189–237.
- [80] C. R. Tracy and K. A. Christian, "Are marine iguana tails flattened?," *Brit. J. Herp.*, vol. 6, pp. 434–435, 1985.
- [81] P. W. Webb, "Form and function in fish swimming," *Sci. Amer.*, vol. 251, pp. 72–82, 1984.
- [82] C. P. van Dam, "Efficiency characteristics of crescent-shaped wings and caudal fins," *Nature*, vol. 325, pp. 435–437, 1987.
- [83] D. Weihs and P. W. Webb, "Optimization of locomotion," in *Fish Biomechanics*, P. W. Webb and D. Weihs, Eds. New York: Praeger, 1983, pp. 339–371.
- [84] H. L. Fierstine and V. Walters, "Studies of locomotion and anatomy of scombrid fishes," *Mem. S. Calif. Acad. Sci.*, vol. 6, pp. 1–31, 1968.
- [85] J. J. Magnuson, "Locomotion by scombrid fishes: Hydrodynamics, morphology and behavior," in *Fish Physiology*, W. S. Hoar and D. J. Randall, Eds. London, U.K.: Academic, 1978, vol. 7, pp. 239–313.
- [86] F. E. Fish, "Power output and propulsive efficiency of swimming bottlenose dolphins (*Tursiops truncatus*)," *J. Exp. Biol.*, vol. 185, pp. 179–193, 1993.
- [87] F. E. Fish and L. D. Shannahan, "Comparative shark locomotion in relation to body and pectoral fin angles," *J. Fish Biol.*, vol. 56, pp. 1062–1073, 2000.
- [88] S. Vogel, *Life in Moving Fluids*. Princeton, NJ: Princeton Univ. Press, 1994.
- [89] R. H. Barnard and D. R. Philpott, *Aircraft Flight*. White Plains, NY: Longman, 1995.
- [90] H. C. Smith, *Illustrated Guide to Aerodynamics*. New York: McGraw-Hill, 1992.
- [91] D. Weihs, "Stability of aquatic animal locomotion," *Cont. Math.*, vol. 141, pp. 443–461, 1993.
- [92] J. E. Harris, "The role of the fins in the equilibrium of the swimming fish. I. Wind-tunnel tests on a model of *Mustelus canis* (Mitchill)," *J. Exp. Biol.*, vol. 13, pp. 476–493, 1936.
- [93] —, "The mechanical significance of the position and movements of the paired fins in the teleostei," *Pap. Tortugas Lab.*, vol. 31, pp. 173–189, 1937.
- [94] —, "The role of the fins in the equilibrium of the swimming fish. II. The role of the pelvic fins," *J. Exp. Biol.*, vol. 15, pp. 32–47, 1938.
- [95] P. W. Webb, "Speed, acceleration and manoeuvrability of two teleost fishes," *J. Exp. Biol.*, vol. 102, pp. 115–122, 1983.
- [96] P. W. Webb, "Designs for stability and maneuverability in aquatic vertebrates: What can we learn?," in *Proc. 10th Int. Symp. Unmanned Untethered Submersible Technology: Proc. Special Session Bio-Engineering Research Related to Autonomous Underwater Vehicles, Autonomous Undersea Systems Institute*, Lee, NH, 1997, pp. 86–103.
- [97] —, "Control of posture, depth, and swimming trajectories of fishes," *Integ. Comp. Biol.*, vol. 42, pp. 94–101, 2002.
- [98] D. Weihs, "Design features and mechanics of axial locomotion in fish," *Amer. Zool.*, vol. 29, pp. 151–160, 1989.
- [99] D. Weihs, "Stability versus maneuverability in aquatic locomotion," *Integ. Comp. Biol.*, vol. 42, pp. 127–134, 2002.
- [100] P. W. Webb, G. D. LaLiberte, and A. J. Schrank, "Does body and fin form affect the maneuverability of fish traversing vertical and horizontal slits," *Environ. Biol. Fish.*, vol. 46, pp. 7–14, 1996.
- [101] F. E. Fish, "Biological designs for enhanced maneuverability: Analysis of marine mammal performance," in *Proc. 10th Int. Symp. Unmanned Untethered Submersible Technology: Proc. Special Session on Bio-Engineering Research Related to Autonomous Underwater Vehicles*. Durham, NH, 1997, pp. 109–117.
- [102] —, "Performance constraints on the maneuverability of flexible and rigid biological systems," in *Proc. 11th Int. Symp. Unmanned Untethered Submersible Technology*. Lee, NH, 1999, pp. 394–406.
- [103] P. P. Wegener, *What Makes Airplanes Fly?*. New York: Springer-Verlag, 1991.
- [104] P. R. Bandyopadhyay, J. M. Castano, J. Q. Rice, R. B. Philips, W. H. Nedderman, and W. K. Macy, "Low-speed maneuvering hydrodynamics of fish and small underwater vehicles," in *Trans. Amer. Soc. Mech. Eng.*, vol. 119, 1997, pp. 136–144.
- [105] P. R. Bandyopadhyay and M. J. Donnelly, "The swimming hydrodynamics of a pair of flapping foils attached to a rigid body," in *Proc. 10th Int. Symp. Unmanned Untethered Submersible Tech.: Proc. Special Session on Bio-Engineering Research Related to Autonomous Underwater Vehicles*. Lee, NH, 1997, pp. 27–43.
- [106] C. M. Breder Jr., "On structural specialization of flying fishes from the standpoint of aerodynamics," *Copeia*, vol. 1930, pp. 114–121, 1930.
- [107] H. H. Hurt Jr., "Aerodynamics for naval aviators," U.S. Navy, NAVWEPS 00-80T-80, 1965.
- [108] D. F. Anderson and S. Eberhardt, *Understanding Flight*. New York: McGraw-Hill, 2001.
- [109] J. A. Walker, "Does a rigid body limit maneuverability?," *J. Exp. Biol.*, vol. 203, pp. 3391–3396, 2000.
- [110] P. W. Webb, "Is the high cost of body/caudal fin undulatory swimming due to increased friction drag or inertial recoil?," *J. Exp. Biol.*, vol. 162, pp. 157–166, 1992.
- [111] F. E. Fish, "Function of the compressed tail of surface swimming muskrats (*Ondatra zibethicus*)," *J. Mamm.*, vol. 63, pp. 591–597, 1982.
- [112] L. A. Ferry and G. V. Lauder, "Heterocercal tail function in leopard sharks: A three-dimensional kinematic analysis of two models," *J. Exp. Biol.*, vol. 199, pp. 2253–2268, 1996.
- [113] W. J. L. Felts, "Some functional and structural characteristics of cetacean flippers and flukes," in *Whales, Dolphins, and Porpoises*, K. S. Norris, Ed. Berkeley: Univ. California Press, 1966, pp. 255–276.
- [114] A. W. English, "Structural correlates of forelimb function in fur seals and sea lions," *J. Morph.*, vol. 151, pp. 325–352, 1977.
- [115] G. D. Fitzgerald, "Comparative morphology of the forelimb skeleton in some Odontoceti (mammalia, cetacea)," M.A. thesis, California State Coll., Long Beach, 1970.
- [116] J. Wyneken, "Sea turtle locomotion: Mechanisms, behavior, and energetics," in *The Biology of Sea Turtles*, P. L. Lutz and J. A. Musick, Eds. Boca Raton, FL: CRC, 1997, pp. 165–198.
- [117] E. J. Slijper, *Whales Ithaca*. Ithaca, NY: Cornell Univ. Press, 1979.
- [118] J. G. M. Thewissen and F. E. Fish, "Locomotor evolution in the earliest cetaceans: Functional model, modern analogues, and paleontological evidence," *Paleobiol.*, vol. 23, pp. 482–490, 1997.
- [119] A. W. English, "Limb movements and locomotor function in the California sea lion (*Zalophus californianus*)," *J. Zool., Lond.*, vol. 178, pp. 341–364, 1976.
- [120] P. E. Purves and G. Pilleri, "The functional anatomy and general biology of *Pseudorca crassidens* (Owen) with a review of the hydrodynamics and acoustics," in *Investigation on Cetacea*, G. Pilleri, Ed. Bern, Switzerland: Inst. Brain Anatomy, 1978, vol. IX, pp. 68–227. Cetacea.
- [121] J. E. Heyning, "Cuvier's beaked whale *Ziphius cavirostris*," in *Encyclopedia of Marine Mammals*, W. F. Perrin, B. Würsig, and J. G. M. Thewissen, Eds. San Diego, CA: Academic, 2002, pp. 305–307.
- [122] G. I. Vasilevskaya, "Structural features of the delphinid pectoral flippers," *Bionika*, vol. 8, pp. 127–132, 1974. translated from Russian.
- [123] G. Pilleri, M. Gühr, P. E. Purves, K. Zbinden, and C. Kraus, "On the behavior, bioacoustics and functional morphology of the Indus river dolphin (*Platanista indi Blyth*, 1859)," *Invest. Cetacea*, vol. 6, pp. 11–141, 1976.
- [124] C. M. Jurasz and V. P. Jurasz, "Feeding modes of the humpback whale, *Megaptera novaeangliae*, in southeast Alaska," *Sci. Rep. Whales Res. Inst.*, vol. 31, pp. 69–83, 1979.
- [125] F. E. Fish and J. M. Battle, "Hydrodynamic design of the humpback whale flipper," *J. Morph.*, vol. 225, pp. 51–60, 1995.

- [126] A. G. Tomilin, *Mammals of the U.S.S.R. and Adjacent Countries*. Cetacea, Moskva, U.S.S.R.: Izdatel'stvo Akademi Nauk SSSR, 1957, vol. IX.
- [127] L. K. Winn and H. E. Winn, *Wings in the Sea: The Humpback Whale*. Hanover, NH: Univ. Press New England, 1985.
- [128] S. M. Minasian, K. C. Balcomb III, and L. Foster, *The World's Whales*. Washington, D.C.: Smithsonian, 1984.
- [129] H. E. Winn and B. L. Olla, *Behavior of Marine Animals*. New York: Plenum, 1979, vol. 3.
- [130] S. F. Hoerner, *Fluid-Dynamic Drag*. Brick Town, NJ, 1965. Published by the author.
- [131] R. W. Blake, "Influence of pectoral fin shape on thrust and drag in labriform locomotion," *J. Zool., Lond.*, vol. 194, pp. 53–66, 1981.
- [132] F. E. Fish, J. Hurley, and D. P. Costa, "Maneuverability by the sea lion, *Zalophus californianus*: Turning performance of an unstable body design," *J. Exp. Biol.*, vol. 206, pp. 667–674, 2003.
- [133] T. G. Lang, "Hydrodynamic analysis of dolphin fin profiles," *Nature*, vol. 209, pp. 1110–1111, 1966.
- [134] S. V. Pershin, *Fundamentals of Hydrobionics*, Sudostroyeniye Publ., Leningrad, Russia, 1988. translated from Russian.
- [135] R. von Mises, *Theory of Flight*. New York: Dover, 1945.
- [136] V. V. Pavlov, "Wing design and morphology of the harbor porpoise dorsal fin," *J. Morph.*, vol. 258, pp. 284–295, 2003.
- [137] J. Lighthill, "Introduction to scaling of aerial locomotion," *Scale Effects in Animal Locomotion*, pp. 365–404, 1977.
- [138] W. Y. Yasui, "Morphometrics, hydrodynamics and energetics of locomotion for a small cetacean, *Phocoena phocoena*, (L.)," M.Sc. thesis, Univ. Guelph, Guelph, ON, Canada, 1980.
- [139] T. G. Lang and K. Pryor, "Hydrodynamic performance of porpoises (*Stenella attenuata*)," *Sci.*, vol. 152, pp. 531–533, 1966.
- [140] D. Küchermann, "The distribution of lift over the surface of swept wings," *Aero. Quart.*, vol. 4, pp. 261–278, 1953.
- [141] J. Ashenberg and D. Weihs, "Minimum induced drag of wings with curved planform," *J. Aircraft*, vol. 21, pp. 89–91, 1984.
- [142] P. Liu and N. Bose, "Propulsive performance of three naturally occurring oscillating propeller planforms," *Ocean Eng.*, vol. 20, pp. 57–75, 1993.
- [143] N. Bose, J. Lien, and J. Ahia, "Measurements of the bodies and flukes of several cetacean species," in *Proc. R. Soc. Lond. B*, vol. 242, 1990, pp. 163–173.
- [144] T. L. Daniel, "Forward flapping flight from flexible fins," *Can. J. Zool.*, vol. 66, pp. 630–638, 1988.
- [145] G. A. Stevens, "Swimming of dolphins," *Sci. Prog.*, vol. 38, pp. 524–525, 1950.
- [146] F. G. Wood, *Marine Mammals and Man: The Navy's Porpoises and Sea Lions*. Washington, DC: Robert B. Luce, 1973.
- [147] J. W. Fitzgerald, "Artificial dolphin blubber could increase sub speed, cut noise," *Navy News Undersea Tech.*, vol. 9, pp. 1–2, 1991.
- [148] M. I. Latz, J. Rohr, and J. Hoyt, "A novel flow visualization technique using bioluminescent marine plankton—Part I: Laboratory studies," *IEEE J. Ocean. Eng.*, vol. 20, pp. 147–149, Apr. 1995.
- [149] J. Rohr, M. I. Latz, S. Fallon, J. C. Nauen, and E. Hendricks, "Experimental approaches toward interpreting dolphin-stimulated bioluminescence," *J. Exp. Biol.*, vol. 201, pp. 1447–1460, 1998.
- [150] D. M. Bushnell and K. J. Moore, "Drag reduction in nature," *Ann. Rev. Fluid Mech.*, vol. 23, pp. 65–79, 1991.
- [151] U. M. Norberg, *Vertebrate Flight*. Berlin, Germany: Springer-Verlag, 1990.
- [152] R. S. Shevell, "Aerodynamic anomalies: Can CFD prevent or correct them?," *J. Aircraft*, vol. 23, pp. 641–649, 1986.
- [153] P. Watts and F. E. Fish, "The influence of passive, leading edge tubercles on wing performance," presented at the 12th Int. Symp. Unmanned Untethered Submersible Technology, Durham, NH, 2001.
- [154] P. W. Bearman and J. C. Owen, "Reduction of bluff-body drag and suppression of vortex shedding by the introduction of wavy separation lines," *J. Fluids Struct.*, vol. 12, pp. 123–130, 1998.
- [155] J. C. Owen, A. A. Szewczyk, and P. W. Bearman, "Suppression of Karman vortex shedding," *Phys. Fluids*, vol. 12, pp. 1–13, 2000.
- [156] C. A. Hui, "Maneuverability of the Humboldt penguin (*Spheniscus humboldti*) during swimming," *Can. J. Zool.*, vol. 63, pp. 2165–2167, 1985.
- [157] H. C. Howland, "Optimal strategies for predator avoidance: The relative importance of speed and manoeuvrability," *J. Theor. Biol.*, vol. 47, pp. 333–350, 1974.
- [158] D. Weihs, "Effects of swimming path curvature on the energetics of fish motion," *Fish. Bull.*, vol. 79, pp. 171–179, 1981.
- [159] P. Domenici and R. W. Blake, "The kinematics and performance of the escape in the angelfish (*Pterophyllum eimekei*)," *J. Exp. Biol.*, vol. 156, pp. 187–205, 1991.
- [160] P. F. Brodie, "The white whale *Delphinapterus leucas* (Pallas, 1776)," in *Handbook of Marine Mammals*, S. H. Ridgway and R. Harrison, Eds. London, U.K.: Academic, 1989, vol. 4, pp. 119–144.
- [161] C. L. Gerstner, "Maneuverability of four species of coral-reef fish that differ in body and pectoral-fin morphology," *Can. J. Zool.*, vol. 77, pp. 1102–1110, 1999.
- [162] J. L. Holak, F. E. Fish, D. P. Nowacek, and S. M. Nowacek, "High performance turning capabilities during foraging by bottlenose dolphins (*Tursiops truncatus*)," *Mar. Mamm. Sci.*, vol. 20, pp. 498–509, 2004.
- [163] P. W. Webb, "The effect of size on the fast-start performance of rainbow trout *Salmo gairdneri*, and a consideration of piscivorous predator-prey interactions," *J. Exp. Biol.*, vol. 65, pp. 157–177, 1976.
- [164] D. Miller, *Submarines of the World*. New York: Orion, 1991.
- [165] R. W. Blake, L. M. Chatters, and P. Domenici, "Turning radius of yellowfin tuna (*Thunnus albacares*) in unsteady swimming manoeuvres," *J. Fish Biol.*, vol. 46, pp. 536–538, 1995.
- [166] F. J. Hester, J. R. Hunter, and R. R. Whitney, "Jumping and spinning behavior in the spinner dolphin," *J. Mamm.*, vol. 44, pp. 586–588, 1963.
- [167] M. Riedman, *The Pinnipeds: Seals, Sea Lions, and Walruses*. Berkeley: Univ. California Press, 1990.
- [168] R. S. Peterson and G. A. Bartholomew, *The Natural History and Behavior of the California Sea Lion*, 1967. Special Pub. 1, Amer. Soc. Mamm..
- [169] M. Nishiwaki, "General biology," in *Mammals of the Sea: Biology and Medicine*, S. H. Ridgway, Ed. Springfield, IL: C. C. Thomas, 1972, pp. 3–204.
- [170] C. J. Madsen and L. M. Herman, "Social and ecological correlates of cetacean vision and visual appearance," in *Cetacean Behavior: Mechanisms and Functions*, L. M. Herman, Ed. Malabar, FL: R. E. Krieger, 1980, pp. 101–147.
- [171] *Handbook of Marine Mammals*, vol. 3, S. H. Ridgway and R. Harrison, Eds., Academic, London, U.K., 1985, pp. 241–273.
- [172] W. F. Dolphin, "Foraging dive patterns of humpback whales, *Megaptera novaeangliae*, in southeast Alaska: Cost-benefit analysis," *Can. J. Zool.*, vol. 66, pp. 2432–2441, 1988.
- [173] J. H. W. Hain, G. R. Carter, S. D. Kraus, C. A. Mayo, and H. E. Winn, "Feeding behavior of the humpback whale, *Megaptera novaeangliae*, in the western North Atlantic," *Fish. Bull.*, vol. 80, pp. 259–268, 1982.
- [174] F. A. Sharpe and L. M. Dill, "The behavior of pacific herring schools in response to artificial humpback whale bubbles," *Can. J. Zool.*, vol. 75, pp. 725–730, 1997.
- [175] A. Ingebrigtsen, "Whales caught in the North Atlantic and other seas," *Rapp. P.-V. Reun. Cons. Int. Explor. Mer.*, vol. 56, pp. 1–26, 1929.
- [176] J. A. Chamberlain Jr., "Jet propulsion of *Nautilus*: A surviving example of early paleozoic cephalopod locomotor design," *Can. J. Zool.*, vol. 68, pp. 806–814, 1990.
- [177] K. J. Lohmann, A. W. Swartz, and C. M. F. Lohmann, "Perception of ocean wave direction by sea turtles," *J. Exp. Biol.*, vol. 198, pp. 1079–1083, 1995.
- [178] W. F. Walker Jr., "The locomotor apparatus of testudines," in *Biology of Reptilia*. ser. Morphology D, C. Gans and T. S. Parsons, Eds. London, U.K.: Academic, 1973, vol. 4, pp. 1–100.
- [179] T. G. Lang, "Speed, power, and drag measurements of dolphins and porpoises," in *Swimming and Flying in Nature*, T. Y. Wu, C. J. Brokaw, and C. Brennen, Eds. New York: Plenum, 1975, vol. 2, pp. 553–571.
- [180] F. E. Fish and D. R. Ketten, "Examination of three-dimensional geometry of cetacean flukes using CT-scans," *Integ. Comp. Biol.*, vol. 42, p. 1230, 2002.

**Frank E. Fish** received the B.A. degree in biology from the State University of New York (SUNY), Oswego, in 1975 and the M.Sc. and Ph.D. degrees from the Zoology Department, Michigan State University, East Lansing, in 1977 and 1980, respectively.

He is a Professor of Biology at West Chester University, West Chester, PA, where he has been on the faculty since 1980. His research is focused on the energetics and hydrodynamics of aquatic locomotion by vertebrates and has been funded by the National Science Foundation and the Office of Naval Research. Recent projects have included examinations of the evolution of swimming modes in aquatic mammals, energetics and maneuverability of marine mammals, hydrodynamic design of biological control surfaces, and energy conservation by formation movement.

Dr. Fish has appeared on the PBS series *Evolution*, and he has appeared in the BBC production *Walking with Prehistoric Beasts*, which was broadcast on the Discovery Channel.